Freie Universität Berlin
Institute of Geosciences
Degree Programme Geological sciences, B.Sc.

Waveform similarity based earthquake cluster analysis in northern Chile

Bachelor's Thesis

David Lube

1. Supervisor: Dr. Folesky
2. Supervisor: Dr. Kummerow

Submission date: May 8, 2024

Declaration

Unless otherwise indicated in the text or references, this thesis is entirely the product of my own scholarly work.

Berlin, May 8, 2024

.....
David Lube

Abstract

Many subduction zones present some interestingly earthquake patterns, that exhibit similar waveforms. They are called repeaters. The common method to quantify the similarity of all desired earthquakes is cross-correlation. It is based on the calculation of correlation between two waveforms, with a maximum correlation value CC_{max} indicating their overlap, and extending the correlations to a matrix containing all earthquake events. Multiple repeaters, with high CC_{max} values among another, form a repeater series(RES). A different method to identify repeaters is precise relocalization, because earthquakes on the same fault patch rupture in the similar manner. So how close earthquakes are spatially distributed seems to affect their waveform similarity. To test this hypothesis, I compared the waveforms of 6 repeater series, each with 100 neighboring earthquakes waveforms located within a 10 km radius. The datasets I used contain the microseismic catalog by Sippl et al. (2023) with over 180,000 events and the RES selection by Freie Universität's Applied Seismology Group.

Firstly, the datasets had to be filtered by their frequencies to establish comparability and to reduce the influence of noise. I compared the results of a 1-4 Hz bandpass to a 1-10 Hz bandpass in their impact on my results. I accessed the locations of the earthquakes and determined the distance of all neighboring earthquakes towards the center point of the RES. The waveforms were loaded from eight seismic stations included in the CX Seismic Network. Cross-correlations of all earthquake events, corresponding to each RES, were operated and used as the input to create superimposed histograms.

The evaluation of the results shows two different significant peaks. One, commonly occurring peak of low correlation, created by dissimilar time series, and a second peak at very high correlation values. Repeaters and neighboring earthquakes are separated by a CC-gap with a lack of correlation values, which is related to the spatial dispersal. Repeaters are a distinct cluster of similar earthquakes to surrounding earthquakes. However, some close located neighboring earthquakes also demonstrate high similarity towards the repeater cluster. The threshold, poor recording conditions or distorted signals could be possible explanations, that these earthquakes did not meet the repeater conditions.

Zusammenfassung

Innerhalb vieler Subduktionszonen wurden Repeater, also wiederholende Erdbeben auf der gleichen Störungszone nachgewiesen. Repeater haben die Charakteristik ähnliche Wellenformen an seismische Stationen zu liefern. Mithilfe der Wellenform-Korrelation kann man die Ähnlichkeiten zweier Erbeben-Signale berechnen. Die Wellen werden übereinandergelegt und zeitlich verschoben, der maximale Korrelationswert wird herausgenommen und als CC_{max} bezeichnet. Sobald mehrere Erdbeben miteinanderuntersucht werden sollen, kann man die Kreuzkorrelation verwenden, indem die Korrelationen zwischen allen Erdbeben als Matrix aufgespannt werden. Eine weitere Methode ist die präzise Relokalisierung der Erdbeben-Hypozentren, da Erdbeben, die auf der gleichen Störungszone liegen ähnliche Bruchmechanismen haben. Dementsprechend könnte man annehmen, wenn man die beiden Methoden betrachtet, dass die Wellenformähnlichkeit, von der räumlichen Position abhängt. Daher habe ich untersucht, ob benachbarte Erdbeben in kurzer Distanz zu den Repeatern hohe Ähnlichkeiten aufweisen und ob sich Repeater als unterscheidbares Cluster zu benachbarten Erdbeben abheben.

In meiner Analyse habe ich die Wellenformen von 6 Repeater Serien und jeweils 100 benachbarten Erdbeben in dem Radius von 10 km miteinander verglichen. Grundlage für meine Analyse bildeten der über 180.000 Erdbeben umfassende Microseismic Catalog von Sippl et al. (2023), und die RES-Selektierung von der Freie Universität's Applied Seismology Group. Der Microseismic Catalog von Sippl et al. (2023) besteht aus 27 aktiven seismischen Station, die zusammen den CX Seismic Network bilden. Innerhalb meiner Analyse habe ich die aufgenommenen Wellenformen von 8 seismischen Station verwendet.

Zuerst wurden zwei unterschiedliche Frequenzfilter verglichen. Frequenzfilter sind zur Bearbeitung der Signale von Nöten, um eine Vergleichbarkeit in den Histogrammen zu schaffen. Die Histogramme zeigen die Verteilung der Kreuzkorrelation, für die jeweilige Station. Dabei zeigen die Repeater untereinander starke Ähnlichkeiten, während die benachbarten Erdbeben nur geringen Korrelation untereinander und zu den Repeatern aufweisen. Zwischen den Korrelationswerten von Repeatern und benachbarten Erdbeben ergibt sich ein Mangeln an Werten, der sich mit der räumlichen Verteilung deckt. Eine kleine Menge an nah benachbarten Erdbeben schafft es jedoch hohe Ähnlichkeiten zu den Repeatern aufzuweisen aber nicht den Repeater Ansprüchen zu genügen. Weitere Nachbetrachtungen dieser Erdbeben könnte Aufschlüsse über die fehlenden Kriterien bringen.

Contents

Introduction

Repeating earthquakes are in the interest of many researches. They have been shown to be a useful tool for estimating the interplate movement (Igarashi et al. (2003)). In this thesis, I will try to examine if the proposed definition of repeaters as events caused by the creep of a distinct seismic fault holds true and are therefore distinguishable from close-located surrounding earthquakes. By doing so, I will compare the waveforms of 6 preselected RES (repeater series) with 100 neighboring earthquake events in the radius of 10 km to the center point of the RES. The waveforms will be in the form of cross-correlation overlap, therefore two earthquakes each produce an overlap ratio (CC_{max} value).

Before analyzing the results, however, it is important to assess the filter of frequencies that are let through the signal. This filter is necessary to ensure a comparability between events, while also reducing the influence of noise on the signal. In this thesis, I will compare two different filter bands of 1-10 Hz and 1-4 Hz by analyzing their results to the data by means of their waveforms, cross correlations matrices and histograms.

After deciding on the better-adapted filter for the data set, I will conduct cross-correlation calculations at eight seismic stations. As a result, each station provides a histogram of the CC_{max} values, which will be plotted on top of each other. Based on these figures and their results, I will answer the question if repeaters are distinct in their waveform similarity and behavior to other neighboring earthquakes. Furthermore, can repeaters be classified as a cluster of similar earthquakes or are only particular pairs of repeaters similar?

Theory

2.1 Region and Dataset

This thesis covers a study region in northern Chile. The region is limited 18°S to the north, 24°S to the south and 70°W to the west, 66°W to the east.

Due to the existence of major megathrust events, the latest in 2014 and its high seismicity rate, the region achieves special attention. Since 2006 it has been permanently monitored by seismic stations of the IPOC.

In this thesis, I worked with the microseismic catalog of over 180,000 events from 2007 to 2021 by Sippl et al. to the extent of 100 neighboring events for six preselected repeater earthquakes series (RES). The catalog is composed of 27 active seismic stations called the CX Seismic Network. The RES were selected with waveform comparisons by Freie Universität's Applied Seismology Group. If the overlap of two earthquakes reached or exceeded the threshold of 0.95 at least at two stations, both earthquakes were selected as repeaters. Repeaters extend to a repeater series (RES), when multiple repeaters correlations among each other exceed the threshold. They identified a total number of 2254 RES. Out of them, I concentrated my work on six RES, to which Dr. Jonas Folesky compiled a dataset for the p-wave picktime of each repeater earthquake at a certain station. Due to the lack of signals at some stations, the distortion of the seismic signal with increasing distance, and for the clarity of the graphics, I have reduced the number of stations I worked with to eight.

2.2 Overview Northern Chile

In northern Chile, the Nazca Plate converge with the Southern American Plate. The Nazca Plate is an oceanic plate and therefore dips under the less dense continental South American Plate. This submersion is called subduction.

The region exhibits high seismic activity, marking it as one of the planet's most active regions (Sippl et al. (2023)). Tension builds up due to the interlock between the plates while the oceanic plate submerges. At some point, the force exceeds the load capacity of the rock and fracture occurs. The submerging Nazca Plate seems to indicate very high seismicity rates, with the predominant proportion of earthquakes occurring at depths of 80-140 km (Sippl et al. (2023)). A vast amount of them manifest at the coupled plate interface (Figure 2.1). Two mentionable mega-thrust earthquakes in the analyzed time period were the Tocopilla earthquake with $M_{(w)}$ 7.8 in 2007 and the 2014 Iquique earthquake, $M_{(w)}$ 8.1. These main events are located at the slab interface in less than 50km depth and can be seen in the Figure 2.1. In this zone, often called seismogenic zone, coupling occurs between the submerging and overriding plate (Husen et al. (1999)).

At this zone, the seismicity can be divided into three different planes. The first is corresponding to the slab interface and reaching its limit at a depth of 50-55 km. While the other two planes dip at a constant angle of about 20° and reach from depths below 25 km until 80-120 km. (Sippl et al. (2018)).

The relative earth plate movement at the convergence zone reaches $65mm/y$ (Kendrick et al. (2001)). The presence of fluids in the oceanic Nazca plate crust and in the lower continental crust of the South American Plate might be the reason for the high seismic activity within the subduction zone (F. Pasten-Araya et al. (2018)).

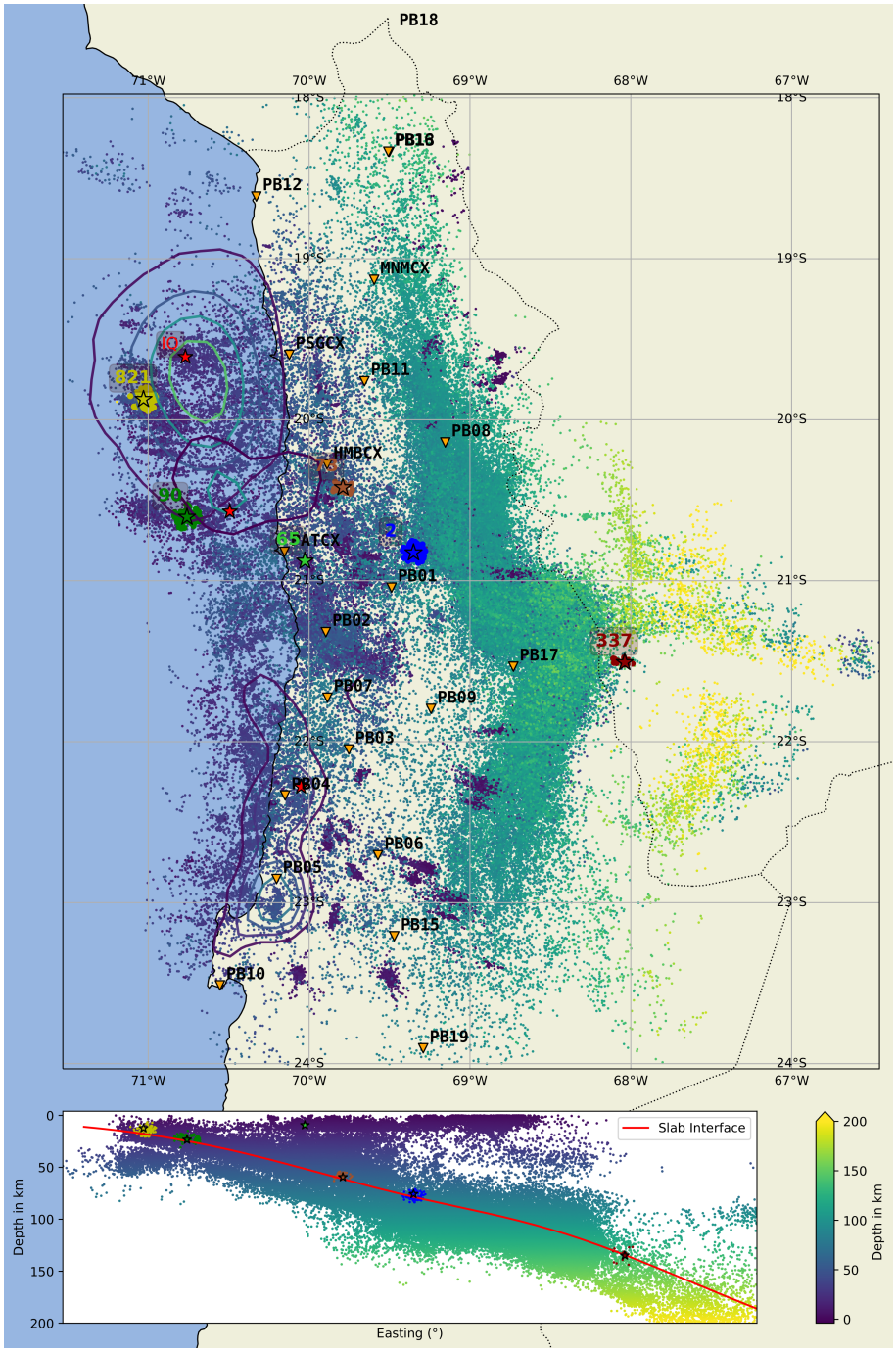

Figure 2.1: Overview of repeaters and surrounding earthquakes. The repeaters are highlighted with stars. Each number stands for the serial number of the repeater series. Stations that compose the seismic catalog are shown as yellow triangles. In the background is the earthquake catalog plotted starting from 2007 to 2021. The earthquakes are scattered with a color map showing their occurring depth.

2.3 Repeating Earthquakes

Repeating earthquakes are reoccurring earthquakes at the same distinct fault patch. They are identical in location and geometry. However, there is no standard definition for repeaters (repeating earthquakes) since the fault area and slip can vary. The magnitude for well-characterized repeaters is mostly small (M<4) however, they can also be of M6 or higher (Uchida and Bürgmann (2019)).

Generally are repeaters interpreted as repeated ruptures of a fault patch loaded with stress from aseismic creep by the fault zone to failure (Uchida (2019)). Figure 2.2 is a model taken from Uchida (2019) to emphasize clarity in the idea of repeating earthquakes.

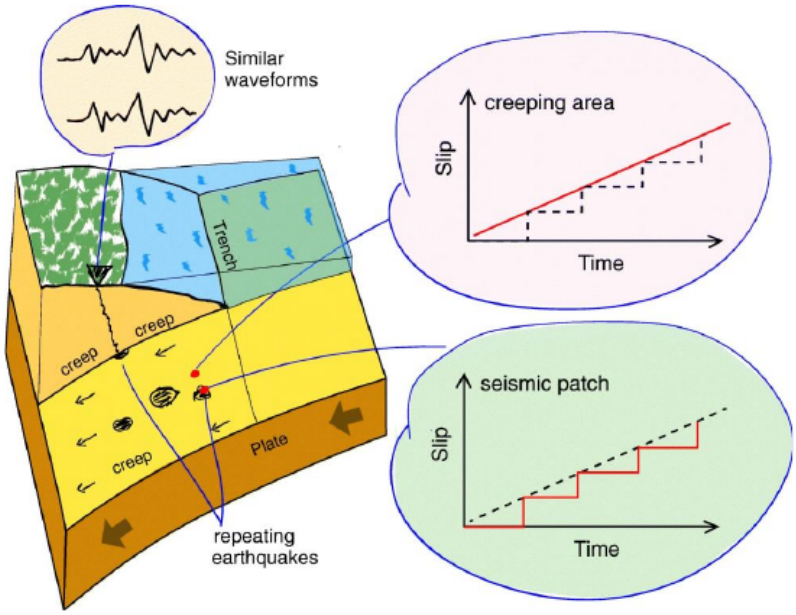

Figure 2.2: Taken from Uchida, 2019. The black nodes represent repeating earthquakes located on seismic patches in the creeping area of a plate boundary. Arrows indicate the movement of the submerging plate and the aseismic creep direction of the fault zone. On the top left are seismic signals shown of repeaters at the same seismic station. Similar waveforms can be observed at the same seismic station because the seismic patches are loaded by creep of the surrounding area and result in ruptures in the same area. The creeping area (top right) and the seismic patch (bottom right) are adjacent and therefore experience almost the same long-term cumulative slip.

Earthquakes in proximity to each other are shown to have similar waveforms. There seem to exist two types. Either very close neighboring earthquakes or co-located earthquakes (repeaters), that share the same fault patch (Uchida (2019)).

There are two common methods for identifying repeaters. One is by precisely relocating the hypocenter of earthquakes by narrowing down the distance between two events. This is done to achieve a higher resolution and to identify if these events are located on the same fault patch. The other, more used and robust version is to compare the waveforms of earthquakes with each other. For this version, the waveforms are cross-correlated and a threshold of the cross correlation value is set to define the repeaters. Because repeaters have no standard definition, the threshold is self-determinable and can vary from scientific work to work, typically it is set to 0.95 Cc_{max}.

2.4 Seismic Waves

Seismic waves are part of the incoming seismic signals by earthquakes received at a seismic station. The total amount of signals contains background noise and arrivals of different seismic waves. A distinction must be made between the two body waves (p- and s-waves) and surface waves. Surface waves have slower velocities and carry more seismic energy. My work will be focused around the body waves. P-wave stands for primary or pressure wave, due to its characterization of being the first wave arriving at the seismic station after an earthquake. Displacement of the particles occurs along the direction of propagation. This wave has the highest velocity of the seismic waves and propagates with:

$$v_p = \sqrt{\frac{K + \frac{4}{3}\mu}{\rho}} \tag{2.1}$$

The second wave arriving at the station is the s-wave, which stands for secondary or shear wave. The particles get displaced orthogonal to the direction of propagation. The velocity of the s-wave can be calculated with:

$$v_s = \sqrt{\frac{\mu}{\rho}} \tag{2.2}$$

Generally, the velocity of p- and s-wave depends on the density of and exerted pressure on the rocks, through which the wave propagates. K stands for the bulk modulus, μ for the shear modulus, and ρ for the density. P-wave velocities range from 5.5 km/s to 12 km/s inside the upper mantle, while s-waves show

velocities from 3.5 km/s to 6.5 km/s (Julian and Anderson (1968)).

In Figure 2.3 the seismic signal of a repeater is displayed. The s-wave shows a higher amplitude than the p-wave, as the s-wave carries more seismic energy.

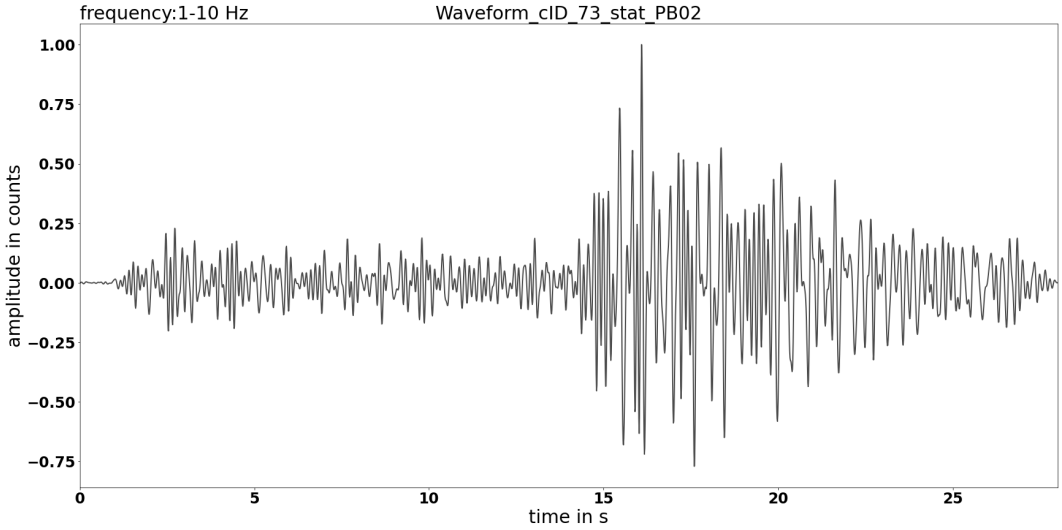

Figure 2.3: This earthquake occurred on the 05th of April in 2014 and belongs to one repeater of the repeater sequence (RES) marked by the serial number 73 recorded at Station PB02. The initial beginning of the seismic movement at the station characterizes the p-wave by arriving first and transporting little seismic energy. At about 15 seconds, the s-wave arrives at the station while creating a much higher amplitude and therefore transporting more seismic energy.

2.5 Cross Correlation

The common method for identifying repeaters is by calculating the cross-correlation coefficient $C(\tau)$ of two time series (here waveforms). The following equation is taken by Uchida (2019).

$$C(\tau) = \frac{1}{N} \sum_{t=1}^{N} f_x(t) f_y(t+\tau) \tag{2.3}$$

Two waveforms f_x and f_y that share the same window length are compared. In the form, that f_y is shifted in time to f_x and the result is a sequence of cross-correlation values for the lag intervals determined by the value of the lag time: τ. The waveforms correspond to the earthquakes x and y with N being the total number of samples (Uchida (2019)).

However, out of this sequence of correlation values, only the highest cross-correlation value CC_{max} in this thesis will be further used. This value is also used to define repeaters and is equivalent to the overlap ratio.
In other terms, the position of two waveforms with the highest similarity is detected, and their correlation contains the CC_{max} value.

Please note, the CC_{max} can vary between -1 (reverse shape) and 1 (identical shape), while 0 indicates no correlation (Gao and Kao (2020)). Of importance for the CC_{max} value is the time frame (window length) and an adequate frequency band (bandpass filter).

2.5.1 Window length

The correlation value of the CC has a high dependency on the window length used for calculating the CC. A shorter window should be more likely to contain higher CC values (Gao and Kao (2020)). Nevertheless, should the window length include both body waves to achieve a detailed comparison. Due to the fact that, for an increased source-receiver distance, the time window has to be increased, attention must be paid to selecting the right window length (Gao and Kao (2020)). I worked with a fixed window length of 28 seconds by considering the arrival time of p- and s-waves to the most amount of seismic stations.

2.5.2 Bandpass filter

A frequency filter for comparing and cross-correlate waveforms is highly suggested among the seismic field.

Not only are frequency filters useful to reduce the effect of noise. Waveforms without a limit at lower frequencies can be unclear to detect overlapping and non-overlapping events. At higher frequencies, plays rupture process variations a greater role for the waveforms. This can even differ between repeaters sharing the same source area (Uchida (2019)).

The filter sharpens the resolution to distinguish between co-located earthquakes (repeaters) and only surrounding earthquakes. To achieve this, it is important to set adequate limits. The frequency band should be careful and with caution applied depending on the source sizes and rupture processes (Uchida (2019)).

Methodology

3.1 Data and Processing

As mentioned at the beginning, I have worked with the compiled microseismic catalog by Sippl et al. (2023) and with the dataset for the RES by Freie Universität's Applied Seismology Group. I examined six RES namely those with the serial numbers 2, 65, 73, 90, 337, and 821. The number of repeaters within the series is approximately consistent, ranging from 20 to 27, only RES-821 and RES-65 stand out, with 55 and 204 Repeaters.

The neighboring earthquakes were limited to a maximum number of 100 Earthquakes within a maximum distance of 10 km to the RES center point. Due to variations in RES locations, as can be seen in Figure 2.1 the number of neighboring earthquakes in close proximity can vary. Although most RES demonstrate a similar distribution, with the 100th earthquake located approximately 9 km away, however two exceptions are worth mentioning. In the case of RES-65, the 100 neighboring earthquakes are located in distances from 0.09 to 0.62 km to the center point, while RES-337 has only 15 neighboring earthquakes within a distance of 10 km. The lack of neighboring earthquakes for RES-337 may be attributed to its location just outside a seismic cloud of many earthquakes. Please note that RES-65 does not fit the common model of repeating earthquakes as explained by Uchida in Figure 2.2 due to not being located at the plate interface.

Eight seismic stations were used to analyze the waveforms: PB02, PB01, PATCX, HMBCX, PB08, PB11, PSGCX, and MNMCX. These are distributed from south to north, covering the closest stations to the six examined RES. The only exception to this is RES-337, where station PB17 and PB09 are located closer than the named stations.

For that reason, the RES-337 histograms consist of nine seismic stations, including also PB09. PB17 lacks hand-picked p-wave arrivals and was therefore not included in this analysis. In general, stations, that are located closer to the RES, achieve a more trustworthy and higher resolution signal due to encompassing the whole p- and s-wave phases. In contrast, stations at greater distances may miss the s-wave phase in the signal

3.1.1 Processing

The neighboring earthquakes were selected by determining a center point of each RES and finding earthquakes within the radius of 10 km to the center point. The waveforms were established by loading the .mseed files contained in the catalog. The miniSEED (mseed) file option is a powerful method for storing large amounts of time series data. In order to load the waveforms of the earthquakes, it was necessary to find the corresponding signals in the seismic catalog. They could be found by detecting the time arrival of the p-wave at a specific station. The p-wave arrival can be calculated by the following equation:

$$t_P = t_o + dt \tag{3.1}$$

t_P stands for the arrival time of the p-wave at a specific station, calculated as the sum of the origin time of the earthquake (t_o) and the travel time to the station (dt). However, the lack of information on the travel time (dt) poses a challenge to calculate the formula. To cope with this problem, Dr. Jonas Folesky provided me hand-picked events and their p-wave arrival time (t_P) at specific stations. The travel time can be assumed to be approximately the same value for repeaters and neighboring earthquakes due to the relatively small distances between them and as followed for RES and neighboring earthquakes per station calculated:

$$dt = t_P - t_o \tag{3.2}$$

The time frame utilized encompasses a buffer of 3 seconds before the p-wave arrival to capture the entire p-wave signal. However, 2 seconds of the buffer had to be stripped, due to the possible influence of unwanted signals. In total, the time frame comprises 28 seconds. To execute calculations and generate figures, I used in this work python 3.9.

The cross-correlation of all events was established by the documentaries from obspy.signal.cross_correlation. Events were correlated by the correlate function and correlation value, shift were saved for the highest overlap using the xcorr_max function (Beyreuther et al. (2010)).

3.2 Procedure

With this processed data, I initially created an ObsPy stream, that included per station the waveforms of RES and their neighboring earthquakes. I used these streams to plot the waveforms, calculate cross-correlation matrices, and eventually plot the histograms. It is important to mention that most of the stations miss some earthquake waveforms due to the lack of their seismic signals at that station. That can vary from station to station and sometimes lead to the result, that some stations lack more than 20 earthquakes in comparison to another station. This can particularly affect the histograms, as the input requires a matrix consisting of CC_{max} values for every earthquake pair. However, such circumstances are mostly exceptional, and reliable stations generally share a similar number of seismic signals. To determine the appropriate pass filter to the data, I applied two different bandpass filters for each process in my analysis and compared the results. The first filter I used has limits of 1-4 Hz, allowing only low frequency signals into the analysis. The second filter has limits of 1-10 Hz. This signal also lets higher frequencies pass and encompassing a broader band. It can be hypothesized that the first filter may increase the CC_{max} values between repeaters and also neighboring earthquakes, but could also amplify the signal-to-noise ratio. The second filter might run into the problem of creating low CC_{max} values between repeaters by taking fracture processes more into account, potentially rendering them undetectable. While on the other hand, it should also be more capable in detecting dissimilarities between two random events.

To determine the most fitting filter for the data set, I will at first compare these pass filters using the waveforms and matrix at one specific station, particular PB01, based on RES-2. The station is located in a close distance to RES-2, as can be seen in Figure 2.1 and thus classifies itself as a good observation point. In addition, PB01 has proven itself in the analysis as a reliable seismic station, providing a well-filled data collection. Finally, I will compare the histograms of RES-2 with both frequency bands. After deciding on a pass band, I will demonstrate the other histograms and conclude whether repeaters and neighboring earthquakes are distinguishable by their waveform similarity and whether repeaters only correlate in pairs or as a cohesive cluster.

3.2.1 Location

RES-2 is located at the plate interface of the submerging and upper plate at depths of about 80 km, marked in blue in Figure 2.1.To provide an overview of the spatial distribution of neighboring earthquakes and repeaters, I generated

a three-dimensional overview of their locations in terms of latitude, longitude, and depth in Figure 3.1. The majority of repeaters and some neighboring earthquakes are localized very close to each other as a spatial cluster, with only two repeaters positioned further away. In contrast, the rest of neighboring earthquakes show a broader spatial, non-contiguous distribution in terms of their location and distance to another. It's essential to consider that this earthquake catalog does not represent a precise localization of every earthquake event, therefore some earthquakes, like the two deviating repeater events could be dislocated.

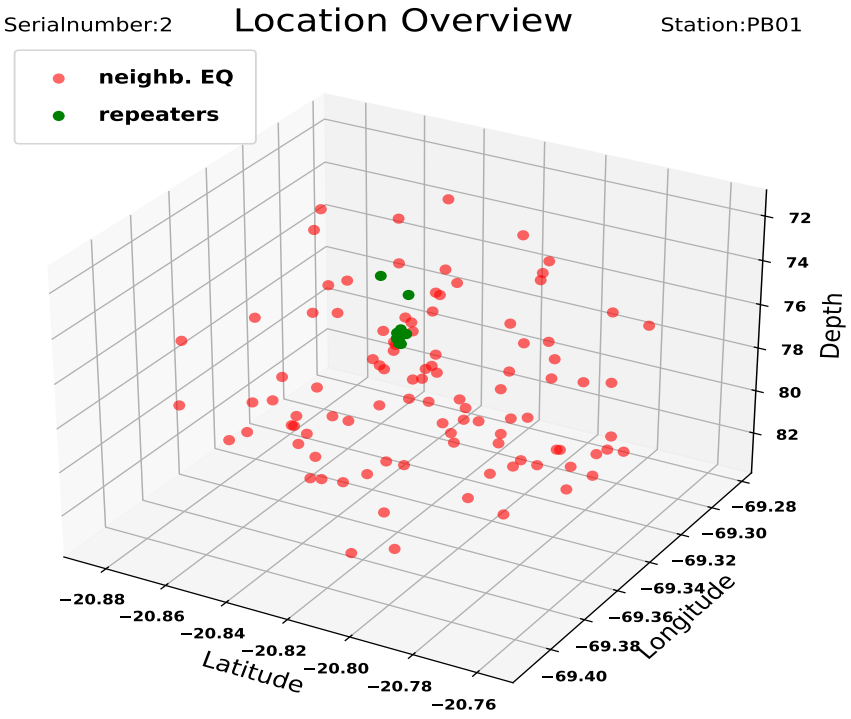

Figure 3.1: The repeaters, in green, are positioned as a spatial cluster, while neighboring earthquakes, in red, are widely scattered across the 10km radius to the center point.

3.2.2 Waveforms

In Figure 3.2 and Figure 3.3, the waveforms of the repeaters and some neighboring earthquakes from RES-2 at station PB01 are depicted. The total number of earthquakes shown in both figures is 50. Please note that the repeaters are not sorted based on their distance to the center point of the RES. Instead, they are arranged based on the occurrence time of the earthquakes, with the oldest seismic signal at the bottom and becoming increasingly younger towards the top. While neighboring earthquakes are sorted based on their distance to the center point, with increasing distance towards the top of the figure.

As can be seen in these figures, some of the first 16 neighboring earthquakes show fairly similar waveforms to the repeaters, even if they have some structural differences. In Figure 3.4 I displayed the waveforms of the 24 neighboring earthquakes located furthest away from RES-2 in my analysis, ranging from about 7 to 8.5 km to the center point. These neighboring earthquakes show little to no similarities to the repeaters. Even when comparing these earthquakes among each other, they exhibit more dissimilarities than similarities. It is to be expected that earthquakes in close proximity show high CC_{max} values between each other, because of sharing with high probability the same or similar source area. In contrast, earthquakes located further away are dissimilar among each other and to the repeaters. Interestingly, the 2 newest repeaters have partially different seismic patterns than the other repeaters in both Figures 3.2 and 3.3. However, this could stem from problems in detecting the proper waveforms at this particular station, PB01. Furthermore, the third-oldest repeater wave shares high similarities to the other repeaters and only lags in time behind.
While comparing the figures 3.2 and 3.3 can be noticed that more information of the signal is transported with a frequency band of 1-10 Hz, due to the more dense seismic signal distribution, than with the 1-4 Hz band. Both methods show the arrivals of p and s-waves in the time frame of 28 seconds. Given the close distance between station and RES center point, the time difference between p- and s-waves is only about 9 seconds.

In the 1-4 Hz pass band, most repeaters achieve higher p-wave amplitudes compared to s-waves, indicating that the p-wave transports more seismic energy. While the s-wave lacks higher frequencies and only appears as a small signal for most repeaters. However, this rule cannot be applied to all earthquakes. Most neighboring earthquakes and the 2 newest repeaters reach higher amplitudes for the s-wave. The low-frequency band makes it challenging to distinguish between low-energy and high-energy rupture processes. For that reason, the body waves are less recognizable as contrasts to the noise in the signal.

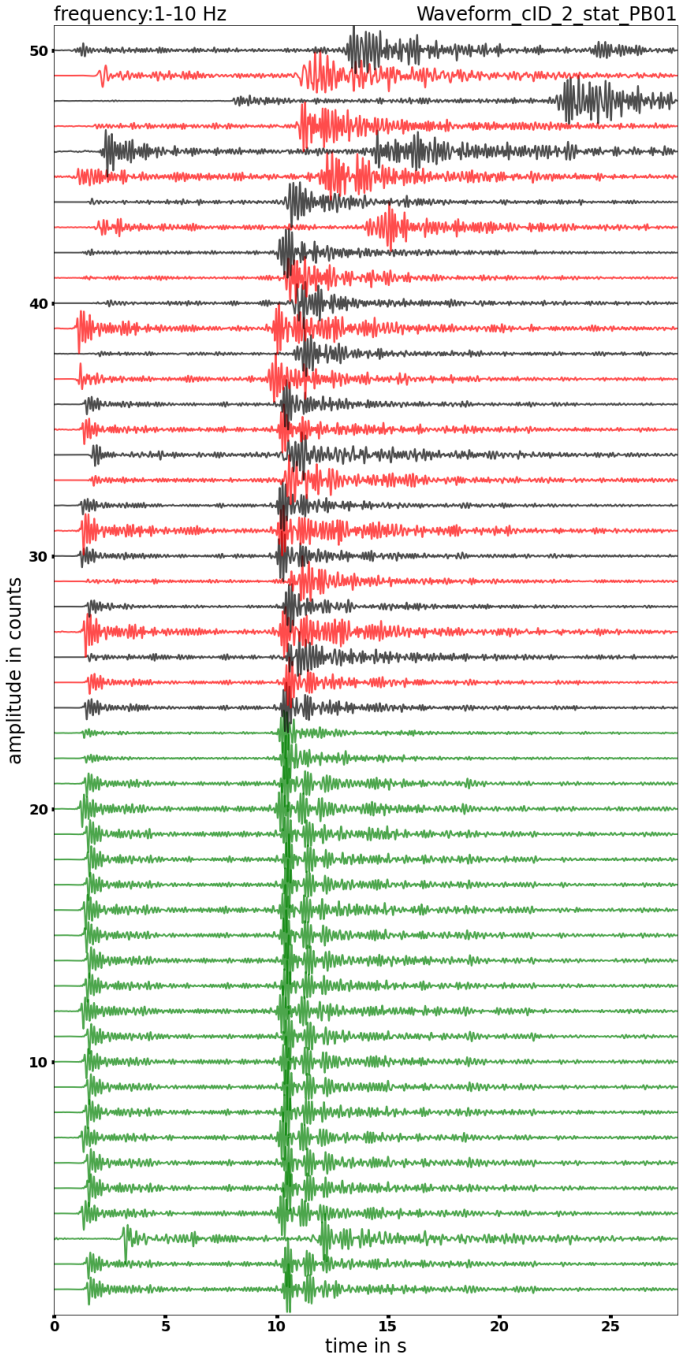

Figure 3.2: 50 loaded waveforms filtered with the pass band of 1-10 Hz. Repeater waveforms, with 23 events, are highlighted in green, while neighboring earthquakes are represented in black and red. The time window covers 28 seconds.

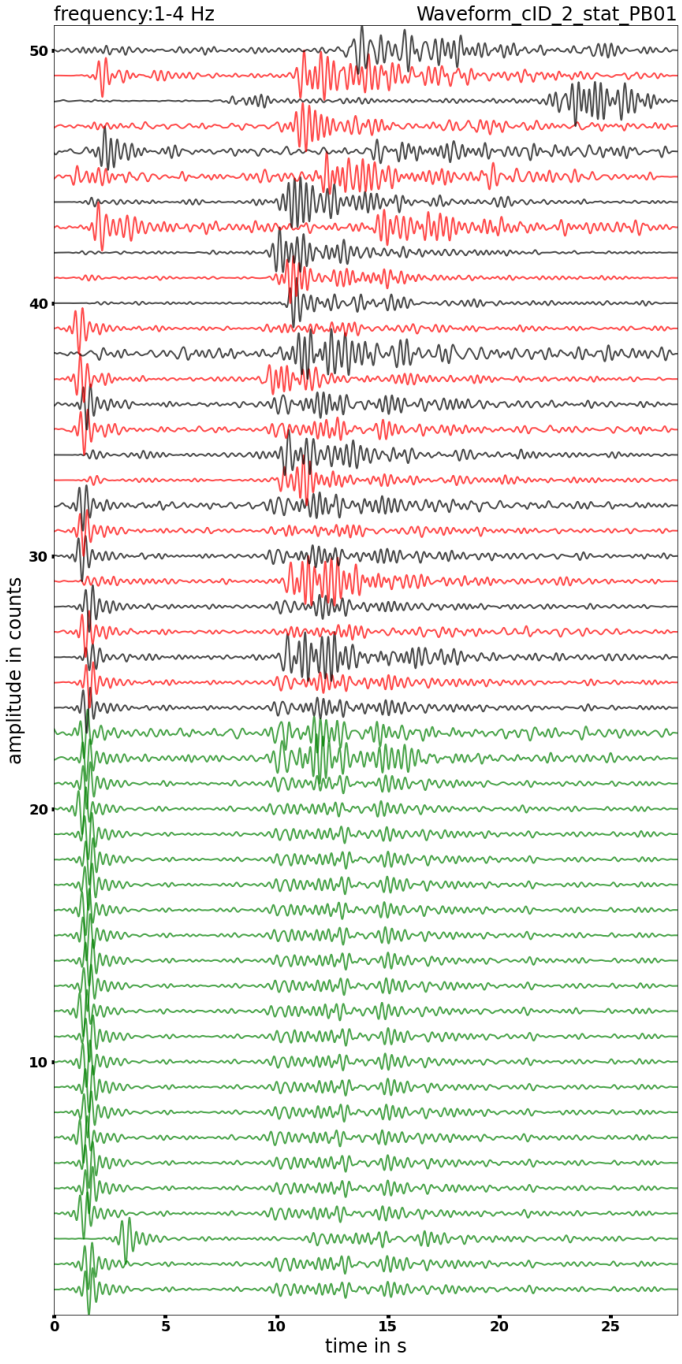

Figure 3.3: As depicted in Figure 3.2, the waveforms from the repeaters are highlighted in green, while those from the neighboring earthquakes are represented in black and red. The applied frequency band covers 1-4 Hz. The wave signals were recorded at station PB01, covering earthquakes from RES-2 or surrounding them.

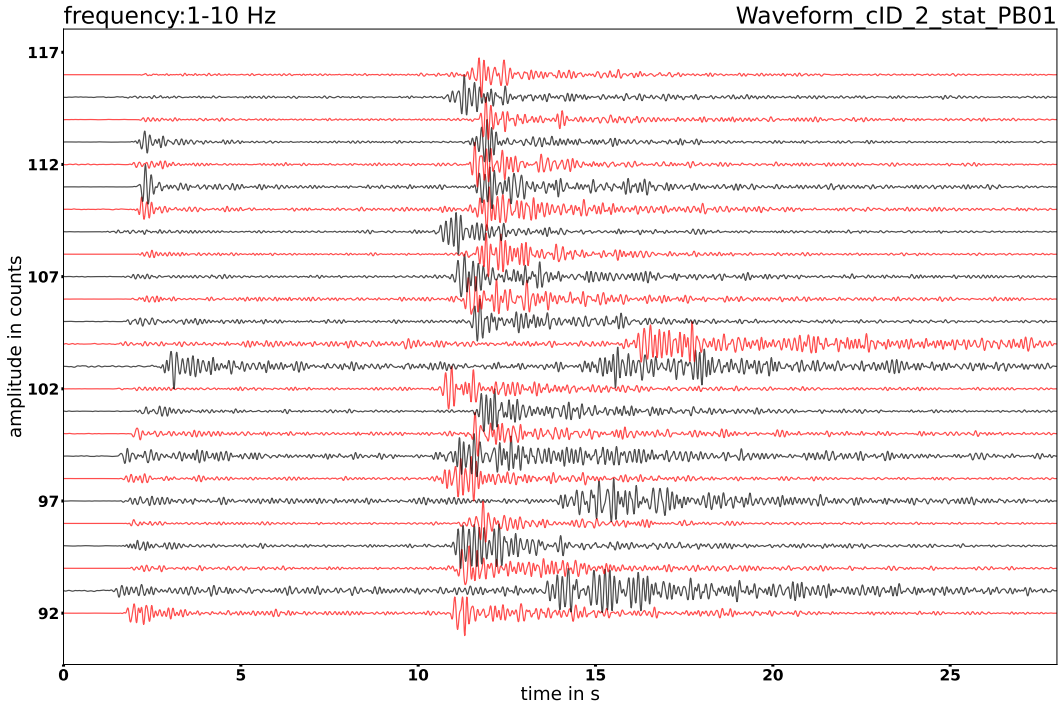

Figure 3.4: These are the waveforms of the 24 neighboring earthquakes recorded at station PB01, situated furthest away from the center point of RES-2.

This becomes especially difficult for detecting the s-wave of the repeaters, they are only slightly prominent to the noise after the s-wave arrival. Therefore, it would be hard for one to determine the end of the s-wave phase.

The pass band of 1-10 Hz enables the possibility of detecting the beginning and end of the s-wave phase by encompassing a broader range of frequencies and increasing s-wave amplitudes in most seismic signals. Notably, the two newest repeaters, which consisted of high p- and s-wave amplitudes in the 1-4 Hz pass band, show reduced s-wave amplitudes and weaker p-wave signals in the 1-10 Hz band. In general, the influence of the p-wave on the total amount of information is reduced by the 1-10 Hz pass band compared to the low-frequency filter.

Between the waveforms, it was to be expected, that the frequency band of 1-10 Hz shows a broader signal distribution, whereas the low-frequency band increases the influence of the p-wave and reduces the influence of the s-wave. The 1-10 Hz pass band provides a clearer distinction between the start and end of p- and s-waves. It also enables a more realistic representation of the seismic energy distribution between p- and s-waves. Furthermore, the 1-10 Hz

band finds the better solution for detecting body waves.

3.2.3 Cross-correlation

The cross-correlation matrix represents the CC_{max} values between all examined pairs of waveforms associated with the RES, received at a given seismic station. Figures 3.5 and 3.6 display these matrices for the two pass bands. While there are overall similarities between the matrices, there are also some minor differences. Each value on the axes in the matrices represents either a repeater or a neighboring earthquake. However, only every 5th event is labeled for clarity. The right side of the Figures is filled by the colorbar, which indicates from purple to yellow the CC_{max} values.

The repeaters are located at the left bottom corner, while neighboring earthquakes extend towards the right and top. The positions of neighboring earthquakes in the matrices figures represent their distance towards the RES center point. The further the neighboring earthquakes extend towards the right and top, the greater the distance to the RES center point becomes. To maintain clarity, are all values transferred into absolute values, although some earthquake pairs reach negative CC_{max} values. However, since the negative values consist of the overlaps with the inverted functions, they show the same correlations as their corresponding positive values. Only values close to zero represent little correlation between two waveforms.

The bottom-left corner is filled by repeaters and their cross correlation with each other, expressing very high CC_{max} values. Close neighboring earthquakes show high similarities to the repeaters as well as to each other, corresponding with the observations made in 3.2.2 Waveforms. However, admittedly, only some of the close located earthquakes show high CC_{max} values, while others share low correlations. The main diagonal with CC_{max} values of 1, crossing from the bottom-left to the top-right, results from the overlaps between the waveforms with themselves, indicating complete correlations. Both matrices show one earthquake situated slightly to the lower left of the center, which has no correlation with any other earthquake. This earthquake lacks its seismic signal at the station and was loaded in as a result of an error in the algorithm. However, this earthquake was excluded in further steps of this analysis. At a certain distance from the RES center point, the cross correlation values from neighboring earthquakes drop significantly and remain approximately the same for earthquake pairs with increasing distance. Both pass bands are capable of detecting the boundary between repeaters and close neighboring earthquakes, as well as between them and distant neighboring earthquakes.

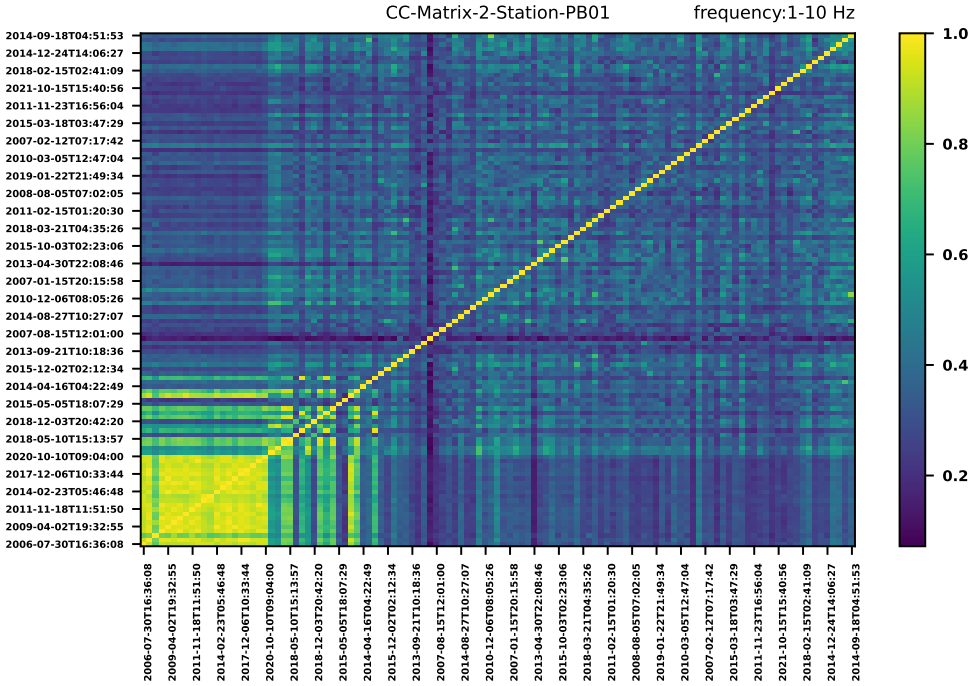

Figure 3.5: The CC-matrix in the frequency band of 1-10 Hz is shown in this figure. The colorbar on the right side indicates the corresponding color to each value in the matrix. The y- and x-axis are labeled with the start time of every 5th earthquake event.The yellow line represents the main diagonal, which results from the overlap between a waveform with itself.

The 1-4 Hz frequency band generally increases the CC_{max} values between earthquakes, especially for the correlations between repeaters, but also some close neighboring earthquakes share high CC_{max} values, ranging from about 0.9 to 0.8 CC_{max}. This is different in the 1-10 Hz filter, where most of neighboring earthquake pairs have lower correlation values ranging at about 0.6 to 0.8, while some exceptions reach values up to about 0.9 CC_{max}. The 1-4 Hz pass band increases the correlations between some distant neighboring earthquakes in comparison to the 1-10 Hz filter. Therefore, some pairs reach CC_{max} values of about 0.8. Interestingly, in both filters, the neighboring earthquakes outside the closely located earthquakes reach higher correlations among each other than with repeaters.

The 1-10 Hz filter enables focusing attention on this particular RES by reducing the overlap of small similarities between further distant neighboring earthquakes. The filter lacks achieving high overlap between every repeater pair, while on the other hand, reducing the correlations to many neighboring

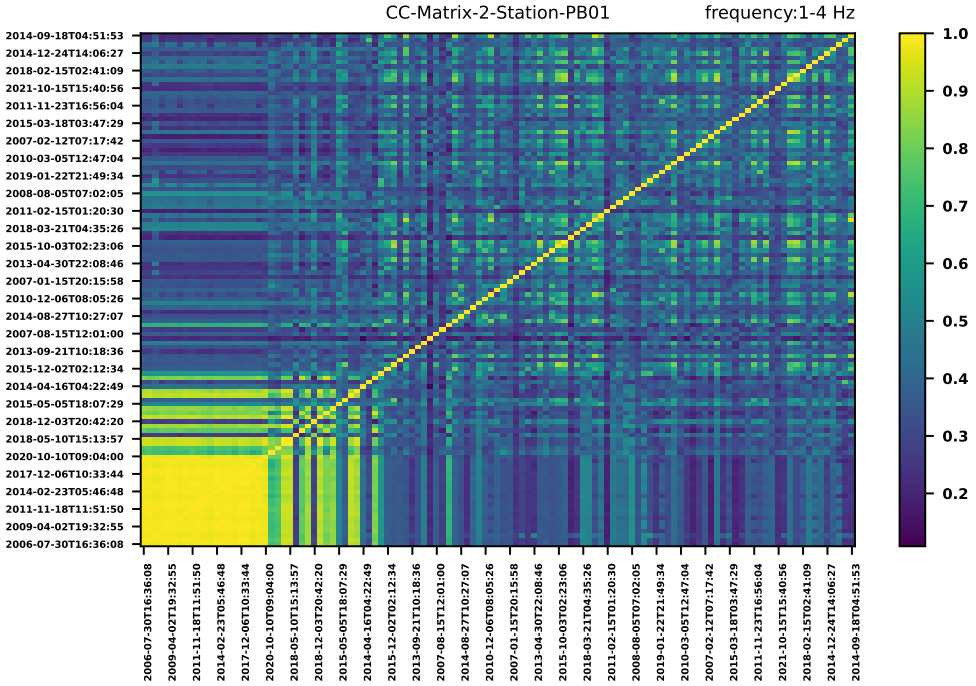

Figure 3.6: The CC-matrix is depicted in the frequency band of 1-4 Hz. This figure indicates very high cross correlation values between repeaters, highlighted in yellow.

earthquakes. To gain a better understanding and find the better-suited band pass, I compared the histograms of RES-2 at the eight previously mentioned seismic stations.

3.2.4 Histograms

The histograms are based on the cross-correlation matrices from the previous section, as well as the matrices from the seven other seismic stations. I displayed the outcome of all of these matrices as histograms on the basis of Igarashi et al. (2003). Figure 3.7 displays the resulting histograms with the pass band of 1-4 Hz, while Figure 3.8 shows the data filtered in frequencies of 1-10 Hz.

The figures display the correlation values on the x-axis and the counts of values on the y-axis. The different colors indicate the stations, sorted from south at the bottom to north at the top. The histograms are superimposed on the frequency count of 100 for the 1-4 Hz pass band and 50 counts for the 1-10 Hz band. The CC_{max} values between the repeaters are plotted in darker shades to differentiate them from values originating in correlations of neighboring earth-

quakes with repeaters or between neighboring earthquakes. Both figures share one clear significant peak in the count of values ranging from 0.2 to 0.4 CC_{max} and a smaller second peak, ranging from 0.95 to 1 CC_{max} in the 1-4 Hz band and from 0.9 to 1 CC_{max} in the 1-10 Hz band. This peak is dominated by correlations between RES, as the same mechanism creates similar waveforms, resulting in high cross-correlation values between them. While some stations are not as reliable as other stations, possible reasons for that will be discussed later in this thesis, for RES-2, most stations deliver well-fitting data.

In comparison, the 1-4 Hz frequency filter with the 1-10 Hz filter, the first exhibit a wider variation of correlation values for the first peak, whereas the second shows a more restricted variance. As mentioned previously, the low frequency band increases the CC_{max} values, resulting in correlations close to 1 between repeaters. However, a significant portion of high correlation values, approximately at 0.9 CC_{max}, results from correlations involving neighboring earthquakes. The matrices and waveforms suggest that these correlations could originate from some close neighboring earthquakes. The 1-10 Hz filter causes a wider distribution of the repeaters, mostly ranging from 0.85 to close to 1 CC_{max}, while also reducing the CC_{max} values of the neighboring earthquakes. This increases the displayed CC-gap in similarity between repeaters and other earthquakes. When correlation values between repeaters reach their lowest point, the value counts drop to a minimum. This can be usually seen at CC_max values of 0.9 or 0.8. At lower correlation values, around 0.8 or 0.7, the count of values increases, usually emerging from the Gaussian distribution of the first peak. I will refer to this phenomenon as the CC-gap.

The distinction of repeaters to neighboring earthquakes in the frequency band of 1-4 Hz is more subtle. It shows no clear visual CC-gap, but the pass band especially demonstrates the high similarity between repeaters by achieving a clearer second peak of them in counts of correlation values than the 1-10 Hz pass band. Thus, the two pass band accomplish in different ways a distinction between repeaters and neighboring earthquakes.

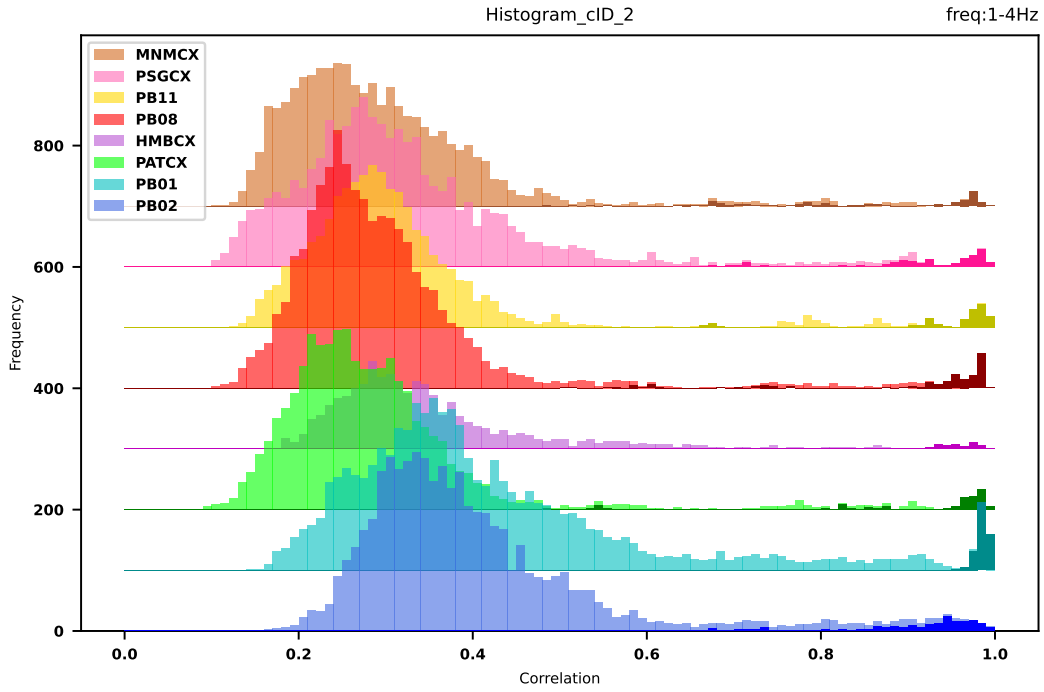

Figure 3.7: This figure shows the histograms with the pass band of 1-4 Hz, different colors represent histograms of different stations. Darker shades of the same color indicate correlations between repeaters. The y-axis is labeled by the counts of correlation values, while the x-axis is labeled by the values of maximum correlation (CC_{max}). Stations PB02, PATCX, PB08, and PB11 show a clear peak of repeater correlations at high CC_{max} values, as indicated by their high counts of correlation values.

Both filters provide a well-fitted resolution of the events and align in their observations across waveforms, cross correlation matrices, and histograms. The low frequency band increases the p-wave signal while reducing the s-wave signal for most repeaters. On the other hand, the higher frequency band enables to include the importance of the s-wave, while also accomplishing a clearer distinction between the body waves and noise. In terms of cross-correlation matrices, the low frequency band generates high CC_{max} values between repeaters, leading to a prominent second peak in the histograms. However, it lacks a CC-gap between neighboring earthquakes and repeaters due to the general increase in correlation between random events.

I prefer the method of using the frequency band from 1-10 Hz because it achieves the cross correlation distinction to neighboring earthquakes with a visual gap, reduces the overlap of two random events, and provides a clearer

recognition of body waves. However, the wider variation of correlation values between repeaters in the 1-10 Hz band is a disadvantage, that has to be considered in the analysis. An important observation from 3.2.3 and 3.2.4 is that some close neighboring earthquakes reach high correlations with repeaters and themselves in both filters. Therefore, these earthquakes achieve correlation values that are otherwise characteristic between repeaters.

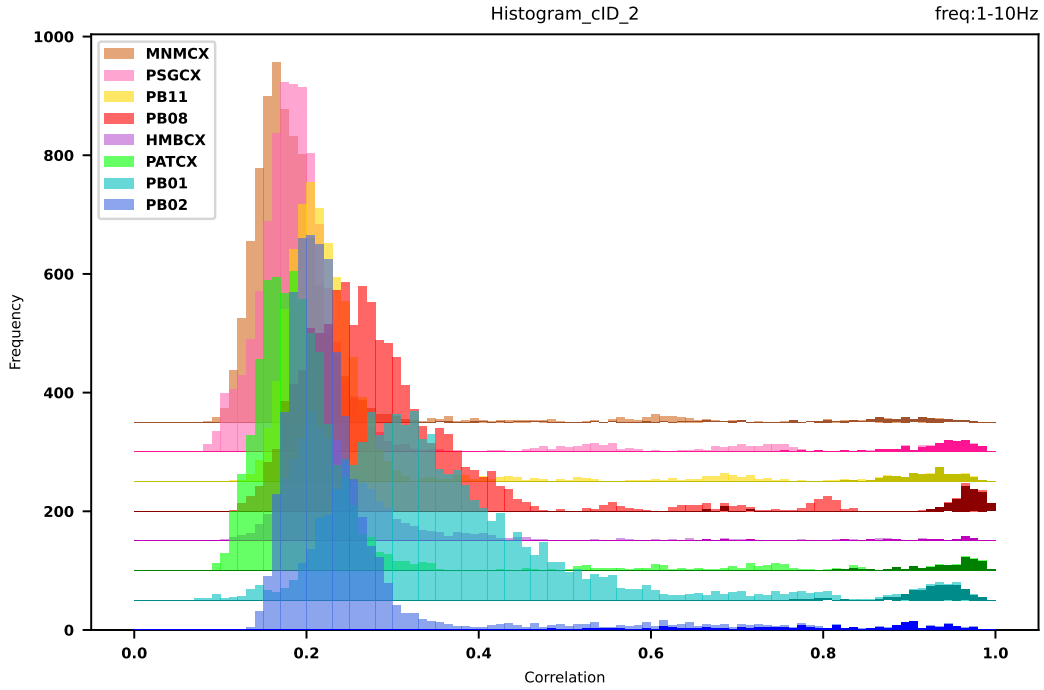

Figure 3.8: In the histograms with the 1-10 Hz pass band, the first peak of frequencies is concentrated on a small range of correlation values. There is a gap in counts of correlation values between repeaters and neighboring earthquakes, which I refer to as CC-gap. Stations PB02, HMBCX and MNMCX do not deliver coherent data to effectively distinguish between repeaters and neighboring earthquakes.

Results

To clarify, I will use the term 'correlation of repeaters' to refer exclusively to correlations among repeaters, and 'correlations of neighboring earthquakes' to refer to correlations between neighboring earthquakes. Correlations between neighboring earthquakes and repeaters mostly occur at lower correlation values and are found within the first peak of the histograms. I will specifically identify correlations originating from closely neighboring earthquakes due to their interesting characteristic of achieving high CC_{max} values.

In Figure 3.8, the cross-correlations of RES-2 for eight stations are plotted. There are notable differences among them. Stations PB02 and MNMCX exhibit a widely dispersed distribution of CC_{max} values for repeaters, ranging from values close to 1 to 0.4 CC_{max}. Conversely, the other stations display a clear pattern, with repeater values ranging from 0.9 to 1 CC_{max}, indicating high overlap among them. Particularly, stations PB01, PB11, and PB08 show a distinct CC-gap between repeaters with high correlation values compared to neighboring earthquakes. The first and largest peak in the histograms corresponds to signals with minimal similarity, reaching correlation values of about 0.1 to 0.3 CC_{max}. As mentioned in the previous chapter, it is expected that if stations provide reliable data, closer stations should be more capable of achieving higher resolution signals. The four closest stations to RES-2 are PB02, PB01, PB08, and MNMCX. However, MNMCX and PB02 are mostly unreliable in delivering coherent data, while PB01 and PB08 exhibit the clearest distinction between repeaters and neighboring earthquakes for RES-2. They also include some correlations of closely neighboring earthquakes at high CC_{max} values.

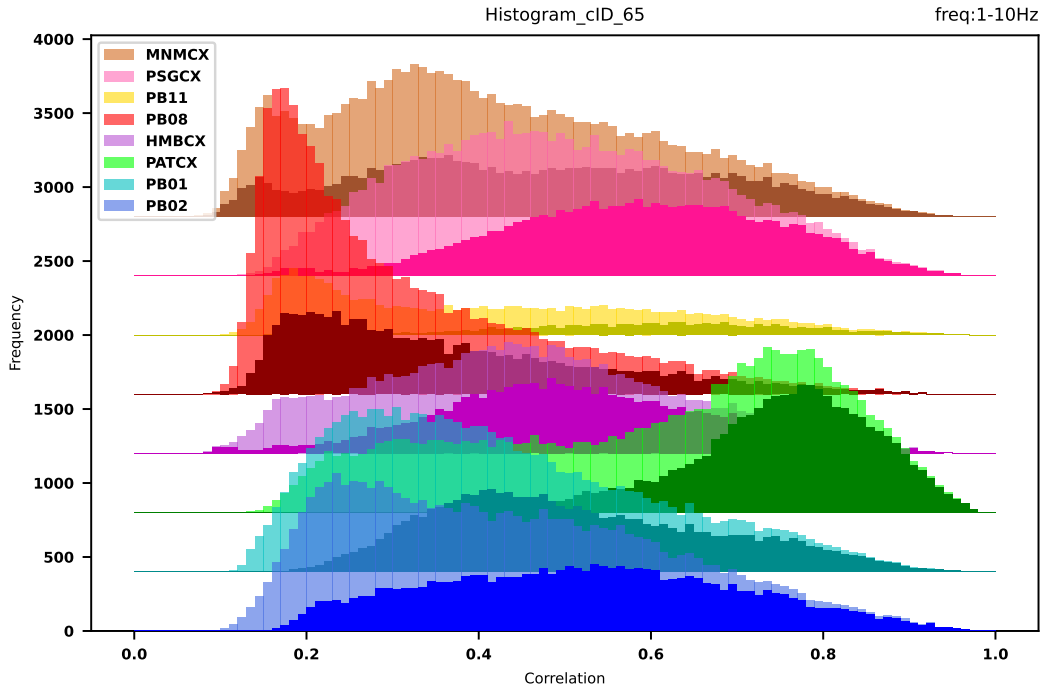

Figure 4.1: RES-65 stands out as an exception compared to RES. The histograms depict a confusing distribution of correlation values, where repeaters and neighboring earthquakes largely align in correlation values. However, only station PATCX predominantly shows repeaters with high correlation values. Conversely, station PB08 exhibits the highest count of repeaters and neighboring earthquakes at low correlation values.

RES-65 stands out as an outlier compared to other RES in terms of both location and the number of repeaters. Unlike earthquakes occurring at the slab interface, those in RES-65 take place in the upper plate of subduction at shallow depths of approximately 10 km. This RES is characterized by 204 repeaters and 100 neighboring earthquakes. Hence, that the region is located in a big cloud of earthquakes, the 100 neighboring earthquakes only reach into a distance of 0.62 km to the RES center point. The correlation analysis of the repeaters presents a complex distribution of CC_{max} values, ranging from 0.1 at certain stations to nearly 1. Consequently, RES-65 does not exhibit a clear distinction in behavior between repeaters and neighboring earthquakes, as they often display similar correlation values. The histograms are dominated by one single peak, with numerous similar counts clustered around low correlation values. The closest station to RES-65, PATCX, primarily shows repeaters with high correlation values. Other stations share the majority of repeaters in low correlation values of about 0.5, with only a small fraction ex-

hibiting high correlation values. In this regard are stations PB11, PB01, PB02, HMBCX, PSGCX similar. An interesting behavior emerges at station PB08, where repeaters and neighboring earthquakes display a significant number of correlations at very low values, approximately 0.2 CC_{max}.

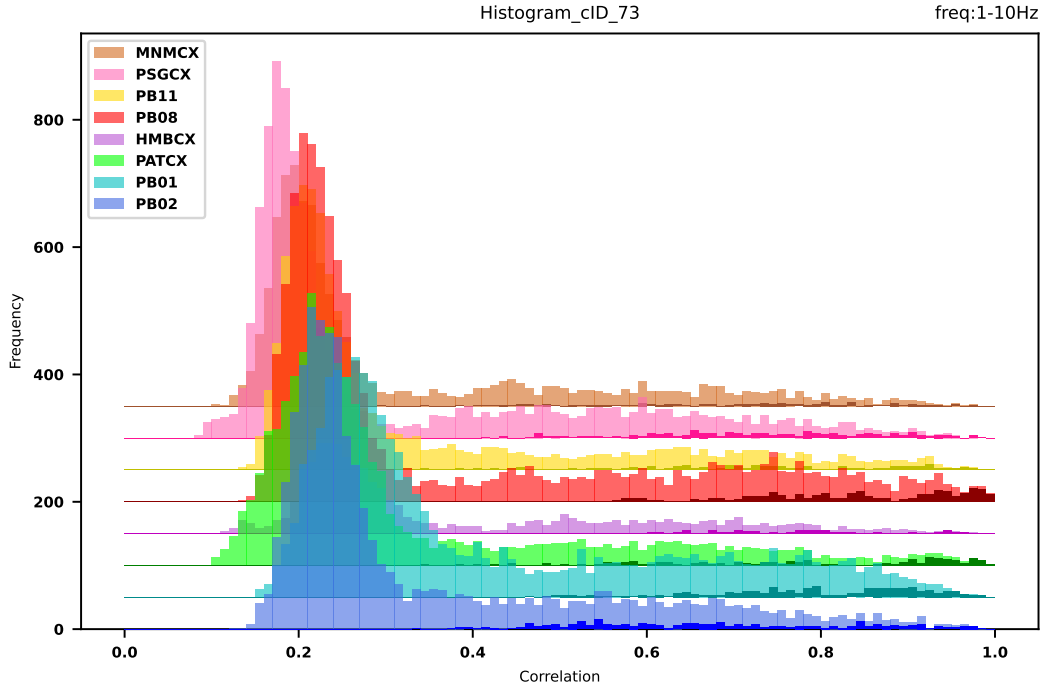

Figure 4.2: The first peak of counts appears at values from about 0.2 to 0.3 CC_{max} across the stations, while repeaters vastly spread from high to medium correlation values.

At 50 km depth is this RES-73 located significantly deeper than previously examined RES. The repeaters vary vastly in correlation values for all stations. Sometimes even reaching as low as correlation values of 0.4 CC_{max}. Significantly, can only one peak be observed, ranging from about 0.2 to 0.3 CC_{max} across the stations. Between correlation values of 0.3 and 0.8 CC_{max}, or even 0.9 CC_{max} in some cases, neighboring earthquakes display similar value counts. The correlations of repeaters vary from high to low values due to reduced cross-correlation of events with the high frequency band. However, this effect should also affect neighboring earthquakes and therefore create a CC-gap if repeaters and neighboring earthquakes should be caused on different seismic patches. Yet, this effect can not be observed in the Figure. The highest correlation values are dominated by repeaters across all stations, although many neighboring earthquakes also reach values close to about 0.9 CC_{max}. However, only station

PB08 and PATCX show a notable concentration of repeater correlation values close to 1. Overall, these histograms do not indicate a clear, distinct image of repeaters compared to neighboring earthquakes.

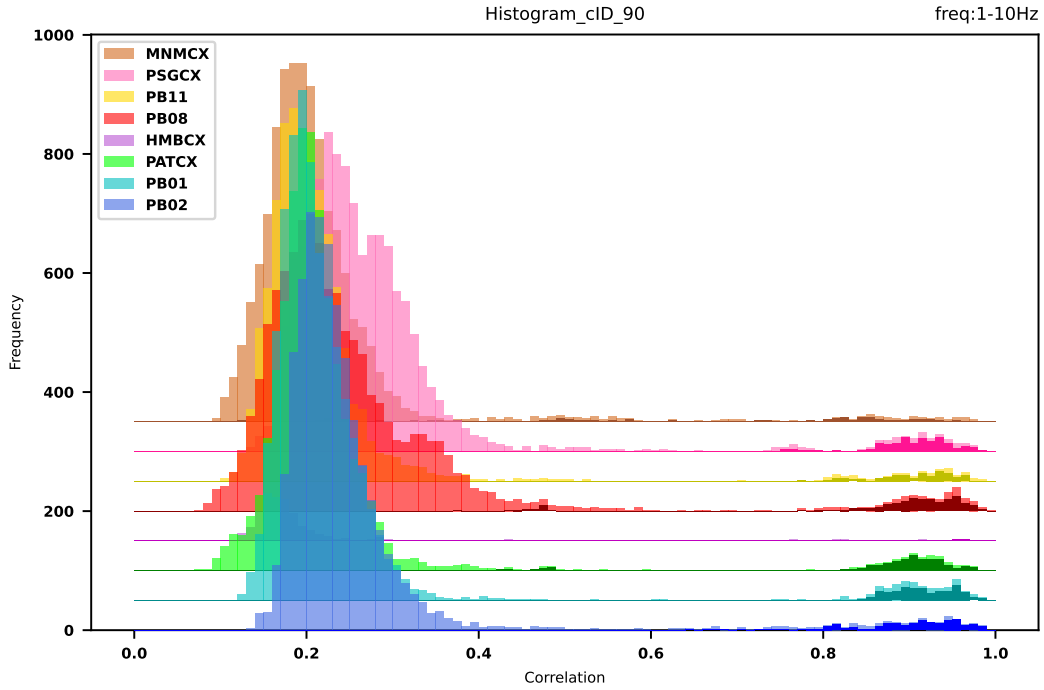

Figure 4.3: At most stations, this RES exhibits a consistent pattern, with two peaks and a noticeable gap in counts between them. Only HMBCX and MNMCX do not show a second peak.

As shown in figure 3.5 the count of correlation values for RES-90 reveal two distinct peaks. The first peak is situated at about 0.2 CC_{max} values, indicating overlaps among time series that share very few similarities. The second peak ranging mostly from 0.85 to close to 1 CC_{max} is highlighted mostly by repeater values but also of some close neighboring earthquake overlaps. Notably, at stations PB08, PATCX, and MNMCX, certain correlations among repeaters show minimal similarity, reaching as low as 0.4 in correlation values. For the stations PB01, PB02, PATCX, HMBCX, PB11 and MNMCX are between 0.4 and 0.8 CC_{max} very few counts of values. This also happens for PSGCX and PB08, although this gap starts slightly later, at around 0.45 to 0.8 CC_{max} values. The CC-gap is the outcome of the dissimilarity between neighboring earthquakes and repeaters. Closest to the RES-90 are the stations PATCX and HMBCX, however HMBCX has received very few seismic signals.

The stations PATCX, PB01, PB02, PB08, PB11 and PSGCX indicate clearly the second peak, which emerges from the correlations of repeaters.

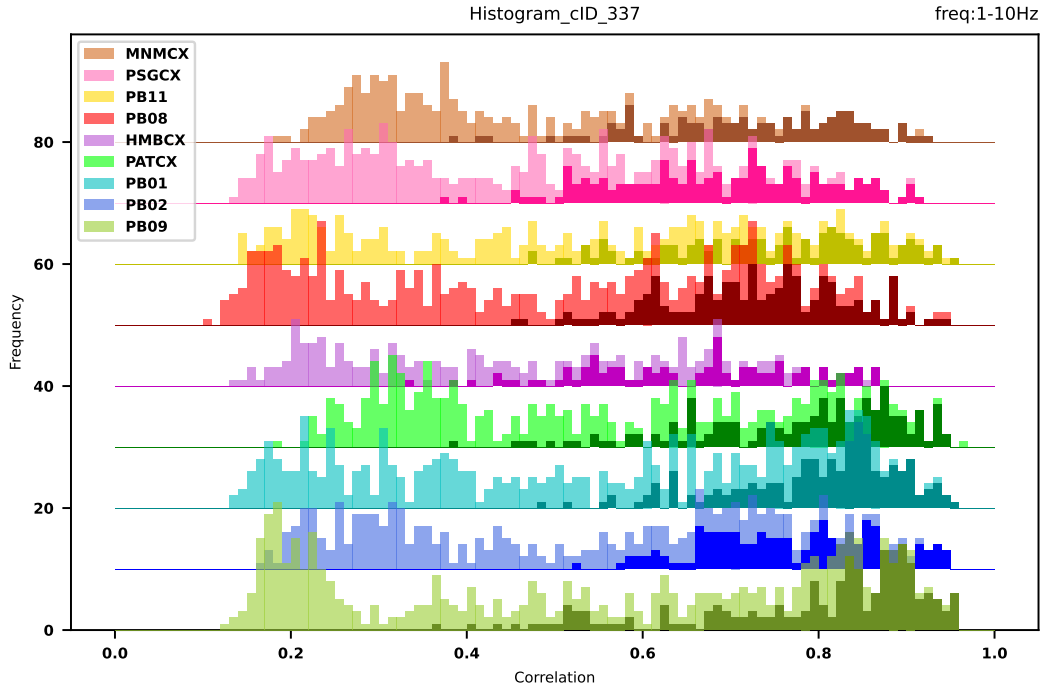

Figure 4.4: There's a high variation of correlation values. The image of the figure could be disturbed due to the low amount of values. However, repeaters generally exhibit higher correlation values compared to neighboring earthquakes.

The RES-337 is located just outside a big cloud of earthquakes. For that reason as mentioned in 3.1 only 15 neighboring earthquakes are included alongside the 20 repeaters resulting in few correlation values. The amount of values can be estimated along the frequency axis, peaking at around 90 counts, while other figures typically range up to 1000 counts. Similar to RES-65 and RES-73, RES-337 also does not show two distinct peaks. The amount of counts is almost evenly distributed along the correlation values of 0.2 to about 0.95 CC_{max}, with high and low correlation values having higher counts than medium correlations. Repeater correlation values mostly range from 0.75 to 0.95 due to their high similarity. The neighboring earthquakes, including close ones, display a wide range of correlation values, from very high cross correlations to low values. Station PB09, located closer to RES-337 than other stations, proves to be the most reliable indicator for repeaters, as it shows the majority of repeater correlations at high values. However, all stations share repeater correlations that show minimal similarity and reach low values. A distinction between

repeaters and neighboring earthquakes is hard to define, as many neighboring earthquakes share high correlation values, and CC-gaps are lacking in the Figure. Even though most repeater correlations reach higher values than those of neighboring earthquakes.

Figure 2.1 shows that RES-821, the last examined RES, is located at shallow depths of approximately 10 km, right at the slab interface. The stations PSGCX, PB11 and HMBCX are located closest to the center point of this RES. Similar to some of the previous histograms, this figure displays two distinct peaks in correlation value counts. The first peak, ranging from cross-correlation values of about 0.2 to 0.3, is characterized by a high number of counts and can be observed at every station. The second peak, however, is only evident at stations PB01, PB11, PSGCX, PB08, PATCX, and MNMCX. It spans from 0.6 to nearly 1 CC_{max} values and is dominated by repeater correlations.

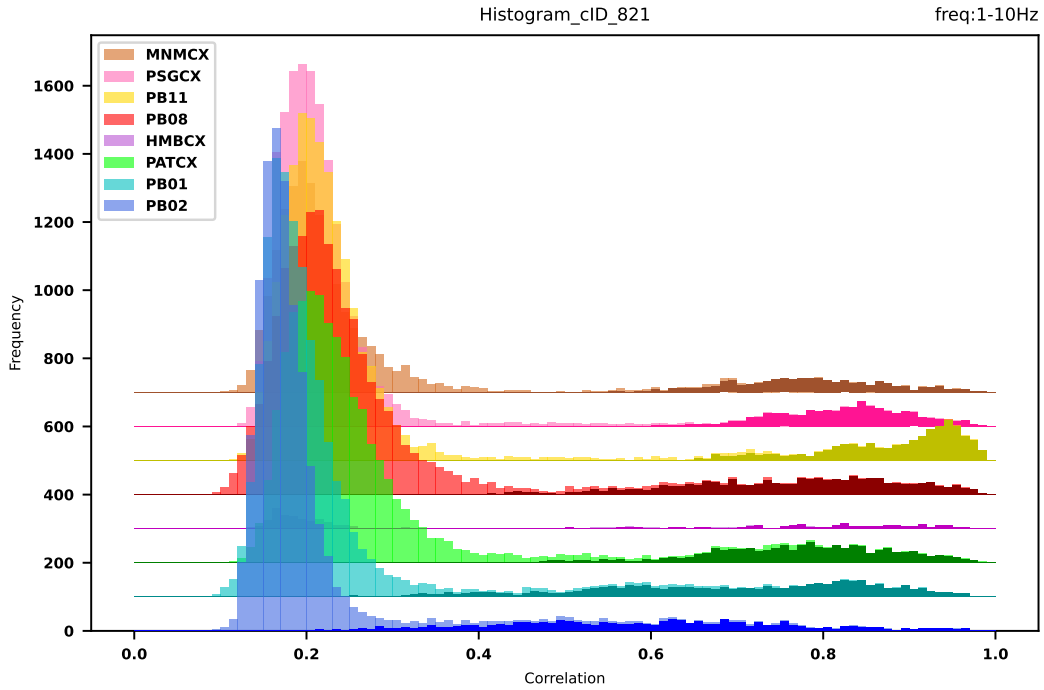

Figure 4.5: There is a distinct first peak around 0.2 CC_{max} values, while the range of the second peak varies from station to station. Repeaters correlation values vary on a long scale, while also dominating the amount of high correlation values. Between the two peaks are few correlation values, creating a CC-gap between repeaters and neighboring earthquakes.

To be emphasized is the station PB11, that achieves a high distribution of repeaters at high correlation values between 0.95 and 1 CC_{max}. The stations HMBCX and PB01 indicate an increase of values at higher correlation values, although their distributions vary considerably and appear relatively flat across increased correlation values. Therefore, they do not indicate a clear second peak at high correlation values. PB02 stands out as the only station without a CC-gap between repeaters and neighboring earthquakes, with repeaters mostly ranging in correlation values from 0.4 to 0.8.

4.1 Repeater distinction

In this thesis, repeaters have been demonstrated to exhibit distinct behavior compared to neighboring earthquakes by prominently featuring a second peak at high correlation values, indicating a high degree of similarity among themselves. Particularly, RES-2, RES-90, and RES-821 appear to show a clear differentiation between randomly chosen neighboring earthquakes and repeaters. Additionally, some close neighboring earthquakes demonstrate a high overlap between each other and with the repeaters. My supervisor Dr. Jonas Folesky has constructed a model to demonstrate the relationships between these earthquake events. Figures 4.6 and 4.7 depict connections between events based on the correlations. Two events that share similar signals are connected by a bond, where the thickness of the bond represents the CC_{max} value. It's important to note that this model is purely illustrative, and the positions of the events do not correspond to their actual geographical locations. For precise locations, refer to figure 3.1, where the model is presented for RES-2 at the same station, PB01, as featured multiple times throughout the thesis. Knots are positioned closer to events with high similarity and further away from dissimilar events. The colors represent the classification or clustering of a particular group of earthquakes. For instance, earthquakes A, B, and C, which share high similarity with each other, are grouped together, while earthquake D, which only has a good correlation with A is marked in a different color.

Figure 4.6 depicts only bonds between repeaters. They are clustered together at a short distance from each other with high connectivity, although some repeaters are located further away from the main cluster. This may suggest that these repeaters show small differences to the main cluster, hence the less intense bonds. However, overall, repeaters demonstrate clear connectivity with every event due to their similar CC_{max} values. It's worth noting that only 21 events are included in the threshold of 0.95, whereas RES-2 at station PB01 contains of 23 repeater waveforms.

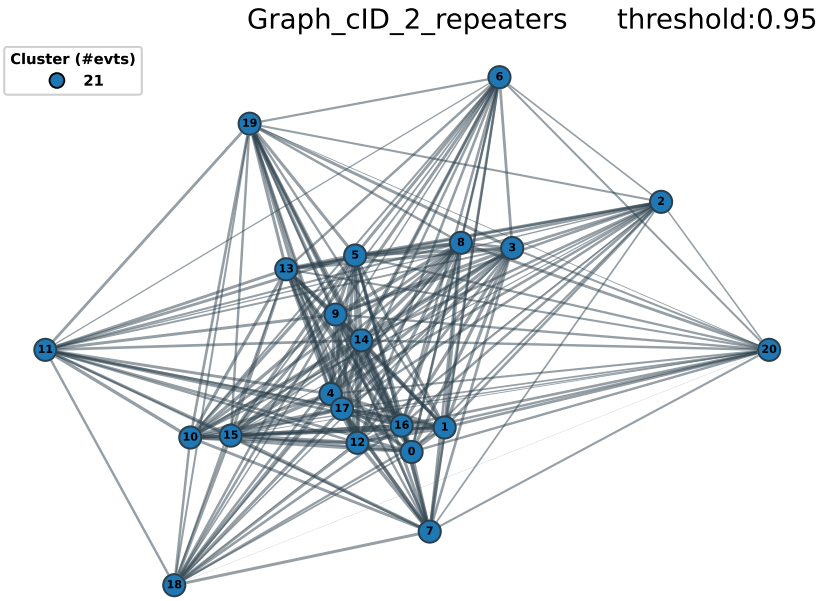

Figure 4.6: Repeaters are captured as knots with bond corresponding in thickness to the amount of correlation value. The threshold of correlation values are limited to a minimum 0.95 CC_{max}. The threshold stands for the lowest limit of correlation values included in this Figure.

The two events not included may correspond to previously identified waveforms that do not entirely fit the correlation structure of the other repeater waveforms at this particular station, PB01.

Figure 4.7 illustrates clustering behaviors among repeaters and neighboring events, considering only correlation values above the minimum threshold of 0.78.

While 20 repeaters create a dense cloud of connectivity in orange, 12 additional events are grouped in the same color, establishing at least some links towards the repeaters. 7 out of 12 events are closely positioned to the cloud and share strong links with it. Presumably, three of these events are the remaining 3 repeaters, likely situated at the top of the repeater cloud in very close proximity to each other. The other non-repeater events in this cluster could be the close situated neighboring earthquakes that share with the repeater group high similarities but were not classified as repeaters. I will refer to this cluster as the high-CC-cluster, because of the high similarity between all earthquakes within the cluster. 21 earthquakes are clustered in blue, showing connectivity among themselves but separate from the repeater cloud. However, their links are fewer and less intense compared to the repeater and close neighboring earthquake cluster. This cluster may arise due to a certain level of similarity based on the amount of data. Events marked in green and red represent pairs sharing links only between each other, indicating a smaller degree of correlation. 59 events couldn't be grouped in a certain cluster and were therefore displayed in the bottom left corner in white.

While repeaters create thick bonds, the majority of neighboring events are dissimilar. The only cluster with multiple bonds formed by the neighboring earthquakes is indicated in blue in Figure 4.7. This cluster, however, lacks high connectivity among their events. Only some of the close neighboring events share a high similarity to the main cloud of repeaters and could be grouped among them. It is important to mention, that these neighboring earthquakes only correspond to a certain extent to the repeaters and were not classified as repeaters due to the threshold and station number criteria.

The high-CC-cluster matches the number of earthquakes located near the RES center point ($<$1 km), as can be seen in Figure 3.1. The rest of neighboring earthquakes is positioned further away and scattered with the 10 km radius. Some of them are clustered, however, the CC-matrix in Figure 3.5 and the histograms do not indicate high similarities among them. The CC-gaps by the histograms correspond to the spatial gap between repeaters and neighboring earthquakes, as only closely neighboring earthquakes around the repeater cluster still reach high correlation values. The other earthquakes have greater distances to the repeaters and lack this high similarity, which means that they only achieve low to medium correlation values.

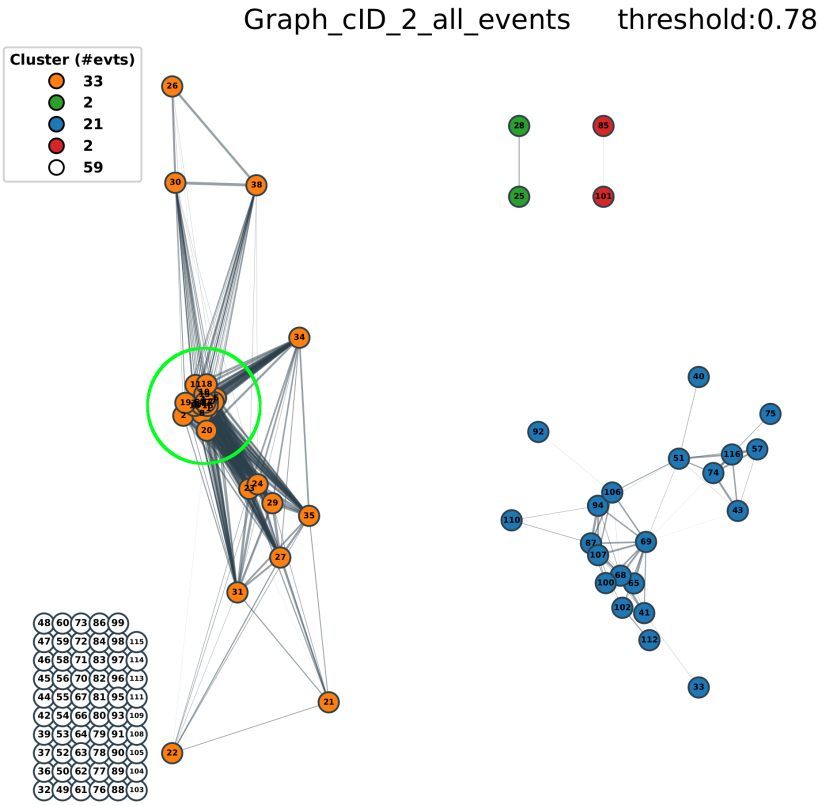

Figure 4.7: This figure contains all correlation values of repeaters and neighboring earthquakes within the threshold of 0.78. Repeaters and close neighboring earthquakes, in orange, form strong bonds, while the rest of neighboring earthquakes mostly do not form bonds. The 21 repeaters shown in the previous figure are circled in green. Those neighboring earthquakes that do form bonds exhibit minimal overlap within the cluster and are also dissimilar to the repeaters.

4.2 Conclusion

Three out of six figures display a clear second peak at high CC_{max} values dominated by repeaters. However, RES-65 and RES-337 pose challenges in drawing conclusions from the results. RES-65 is situated in the upper plate at 10 km depths and therefore does not fit the model proposed by Uchida (2019), where repeaters are localized at the plate interface. Also, the abstrusely high number of repeaters, 204 in total, raises concerns about the validity of observations. On the other hand, RES-337 consists of very few neighboring earthquakes, which could potentially distort the observations due to the low amount of data. Although RES-337 exhibits high correlations values among the majority of repeaters and therefore a distinction to neighboring earthquakes, care must be taken when interpreting the results due to the possible erroneous nature of the data. Excluding RES-65 and RES-337 from further consideration, three out of four figures demonstrate a dominance of high CC_{max} values among repeaters and a CC separation from neighboring earthquakes, with a lack of correlation values mostly around 0.8 CC_{max} - the CC-gap. Therefore, the waveforms of repeaters are distinguishable in similarity to surrounding events. In comparison, between the spatial distribution in Figure 3.1 and the cluster behavior of cross correlation values in Figure 4.7 stands out, that approximately the same number of repeaters and close located neighboring earthquakes, that are connected through the high-CC-cluster are positioned in proximity to another and therefore within the spatial cluster. Hence, the high-CC-cluster matches the spatial cluster. Reasons for this are that the repeaters and close neighboring earthquakes are positioned on the same fracture system that lead to similar stress releases. While the CC-gap corresponds to the spatial gap, as the areas of distant neighboring earthquakes reach only medium correlation values and repeaters reach CC_{max} values close to 1. Therefore, close spatial variations ($<$10km) between repeaters and surrounding earthquakes contribute to their waveform similarities.

On the other hand, particular neighboring earthquakes are positioned in close proximity to another, but do not reach as an earthquake pair a high correlation value. Therefore, the decisive factor for the waveform similarity is not the location but instead the fracture behavior. Repeaters occur according to Uchida (2019) on fault patches that have the same stress releases due to the aseismic creep by the fault zone. While randomly selected neighboring earthquakes, which occur on different dates, can have on the same fault patch very different stress releases, due to their different interlock-states. The location, however, partially coincides with the fracture behavior as earthquakes within the high-CC-cluster are presumably located on the fault zone of the repeaters.

While the more distant earthquakes should be located on fault patches with abrupt stress releases.

Generally, repeaters share mostly high correlation values between each other, ranging from close to 1 to about 0.8 CC_{max}. However, there are exceptions to this pattern at some stations, where repeater correlations vary along the CC_{max} value axis. They may be attributed to seismic interference, technical problems during waveform reception, or signal degradation over increased distances from the source to station. The occurrence of correlation values as low as 0.8 among repeaters is attributed to the pass band. As mentioned previously, the higher frequency band results in reduced correlations among repeaters, as well as decreased similarities between non-well-overlapping events, thus also increasing the CC-gap between repeaters and neighboring earthquakes. Repeaters sharing correlation values of about 0.8 still show high similarities due to the general adjustment of the filter to include rupture process variations to a greater extent.

In the appendix, histograms for the 1-4 Hz pass band illustrate the high similarity among repeaters. The earthquake pairs of repeaters consistently demonstrate high cross-correlation values, as evident in the histograms and the exemplary Figure 4.7, indicating that repeaters not only correlate in a simple sequence of pairs, but rather create a distinct earthquake cluster.

However, certain correlation values, either among neighboring earthquakes or between neighboring earthquakes and repeaters, reach very high correlation values and are situated within the second peak. While examining the matrices and waveforms corresponding to the histograms, I observed that some of these neighboring earthquakes are located very close to the center point of the RES. This can also be seen in Figure 3.5 showing the matrix for the example of RES-2 at station PB01. They show marginally small differences in their cross-correlation values in contrast to the repeaters. If those close neighboring earthquakes should be considered among the repeaters can only be decided by the definition of the repeater series. However, since the repeater definition emphasizes robust signals with very high similarities, I find it appropriate to classify only signals with these prerequisites as repeaters.

Appendix

The histograms for the remaining RES plotted with the 1-4 Hz frequency filter.

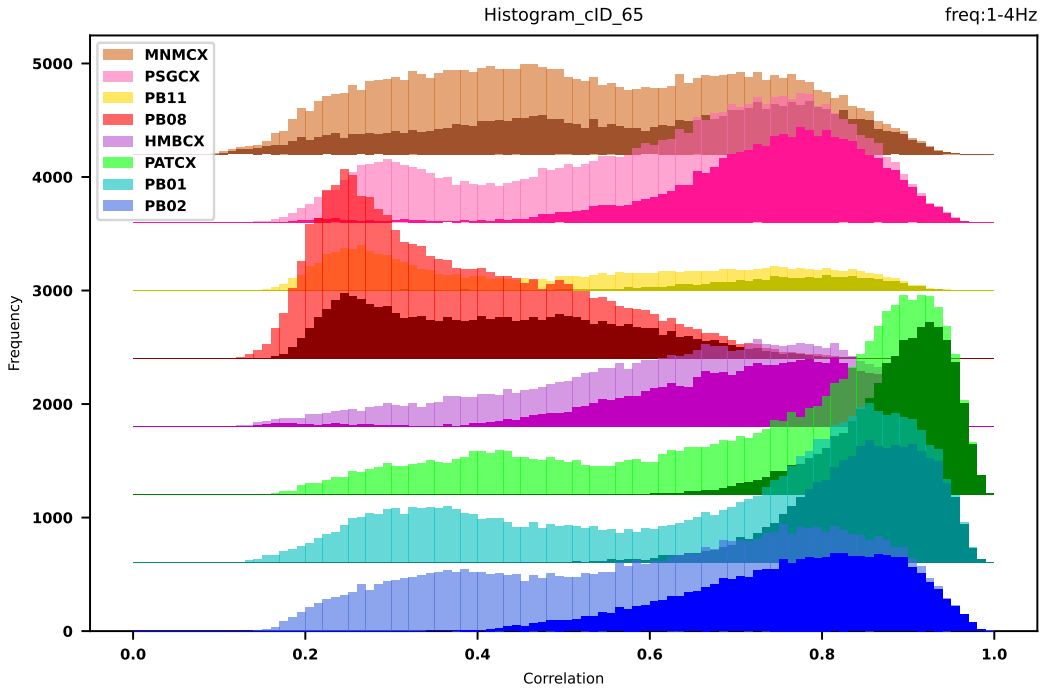

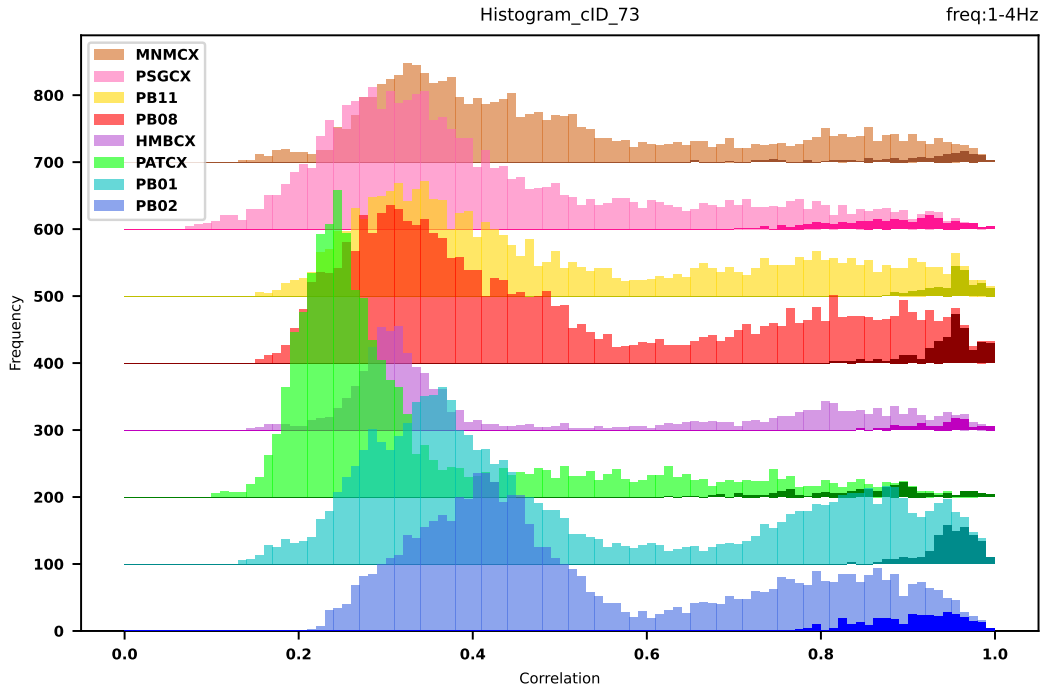
Histogram_cID_73
freq:1-4Hz
MNMCX
PSGCX
PB11
PB08
HMBCX
PATCX
PB01
PB02
Frequency
Correlation
0
100
200
300
400
500
600
700
800
0.0
0.2
0.4
0.6
0.8
1.0

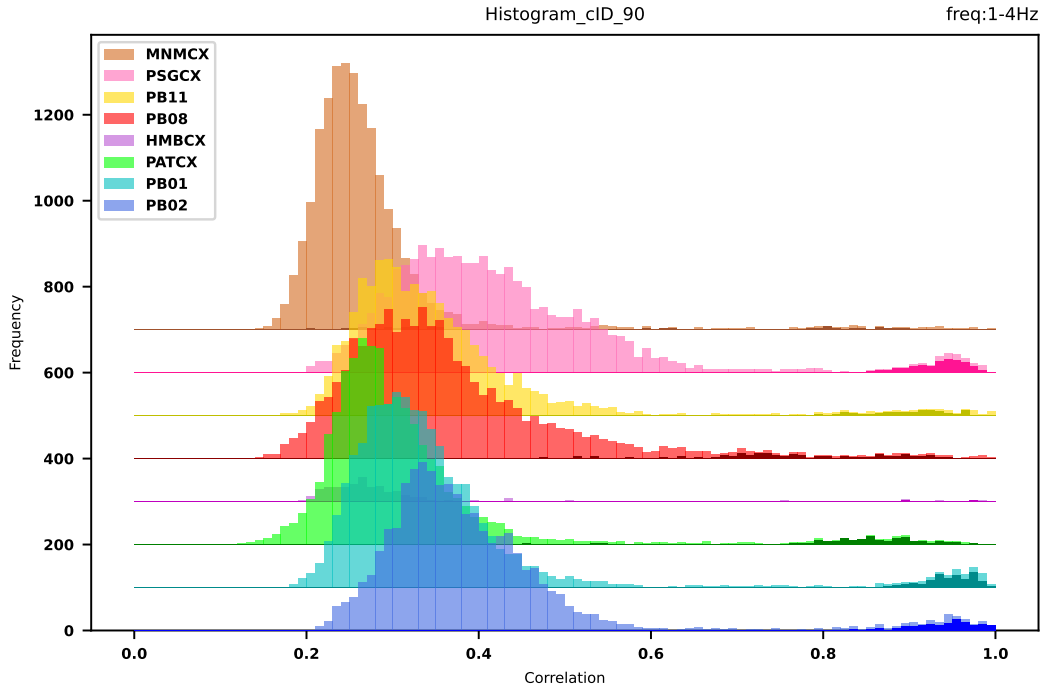
Histogram_cID_90
freq:1-4Hz
MNMCX
PSGCX
PB11
PB08
HMBCX
PATCX
PB01
PB02
Frequency
Correlation
0
200
400
600
800
1000
1200
0.0
0.2
0.4
0.6
0.8
1.0

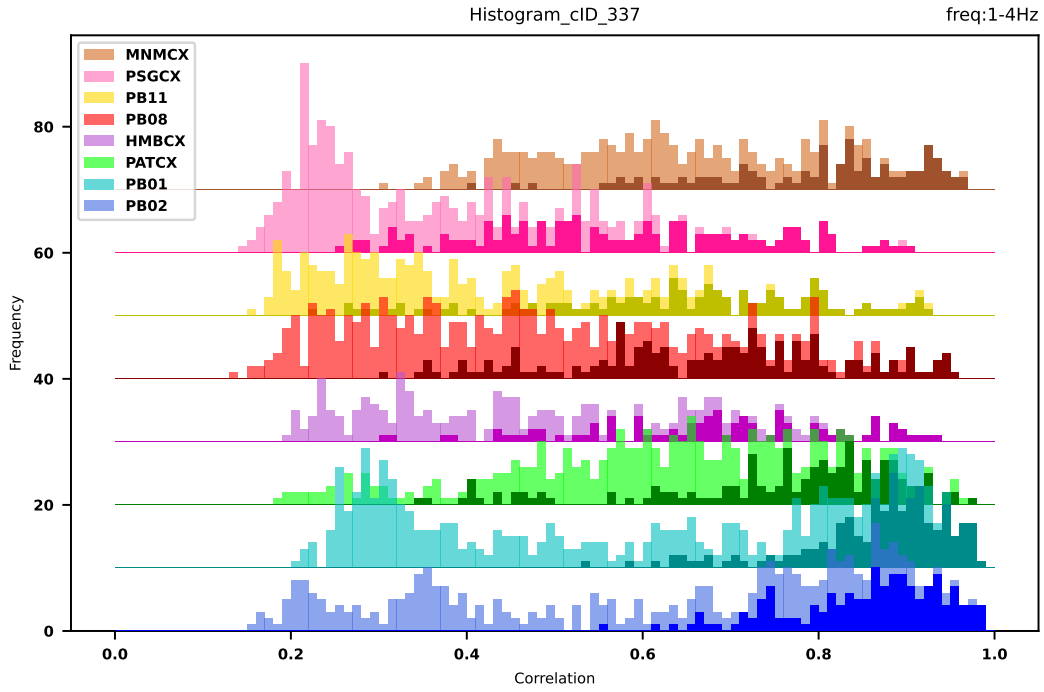
Histogram_cID_337
freq:1-4Hz
MNMCX
PSGCX
PB11
PB08
HMBCX
PATCX
PB01
PB02
Frequency
0
20
40
60
80
0.0
0.2
0.4
0.6
0.8
1.0
Correlation

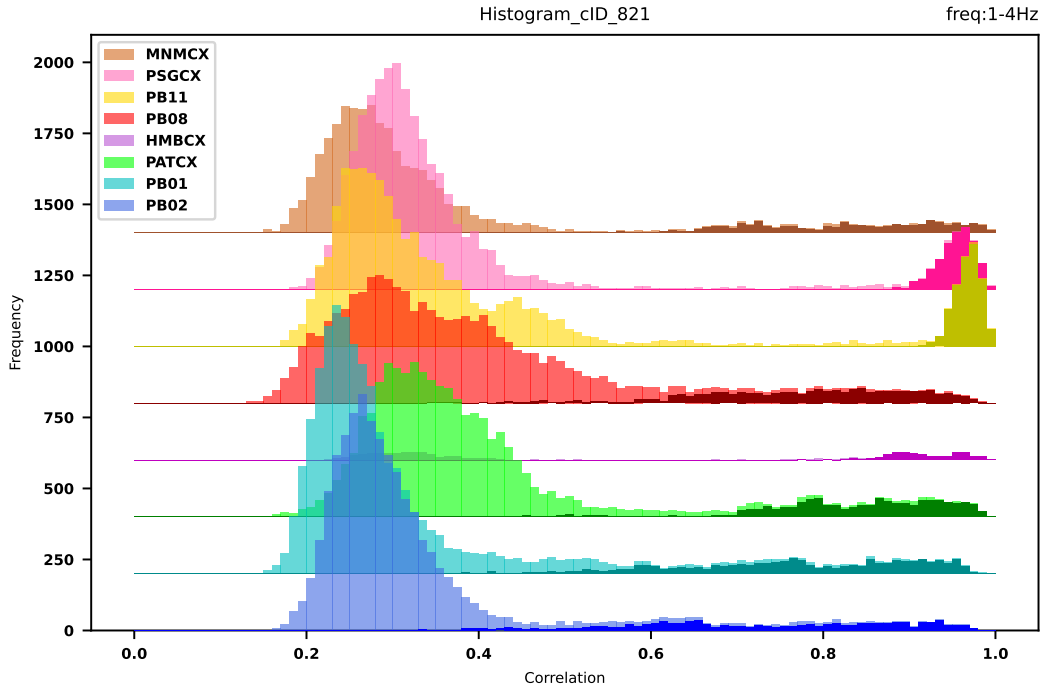
Histogram_cID_821
freq:1-4Hz
MNMCX
PSGCX
PB11
PB08
HMBCX
PATCX
PB01
PB02
Frequency
0
250
500
750
1000
1250
1500
1750
2000
0.0
0.2
0.4
0.6
0.8
1.0
Correlation

Locations of the repeaters and neighboring earthquakes for the remaining RES:

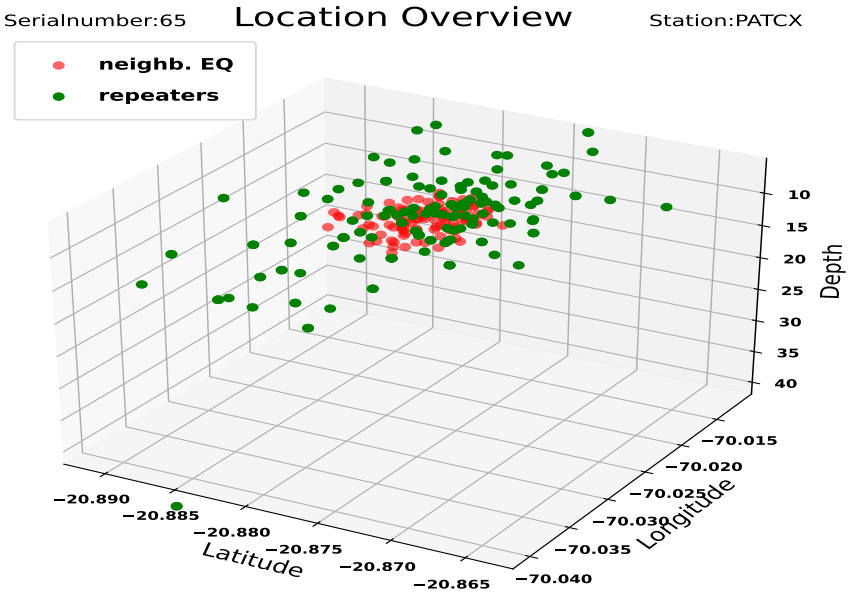

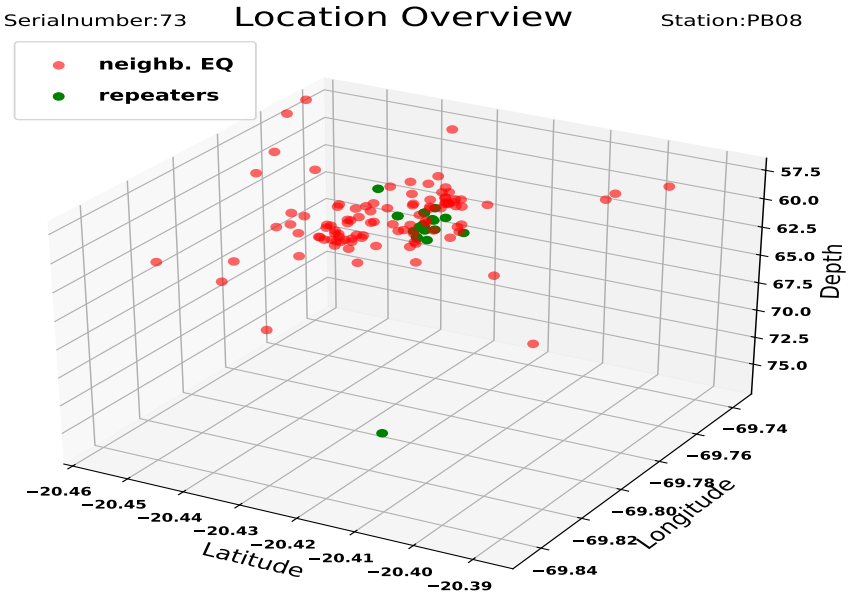

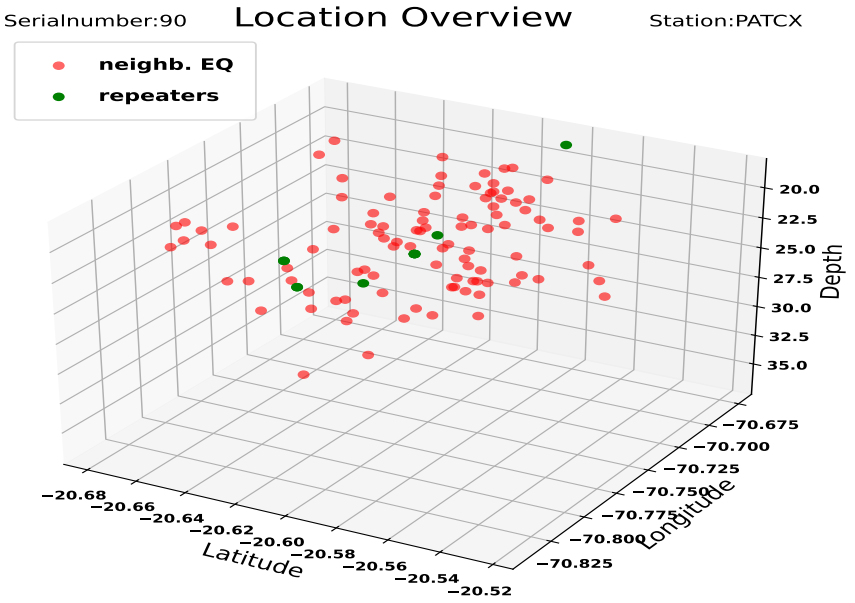
Serialnumber:90
Location Overview
Station:PATCX
neighb. EQ
repeaters
Depth
20.0
22.5
25.0
27.5
30.0
32.5
35.0
Longitude
−70.675
−70.700
−70.725
−70.750
−70.775
−70.800
−70.825
Latitude
−20.68
−20.66
−20.64
−20.62
−20.60
−20.58
−20.56
−20.54
−20.52

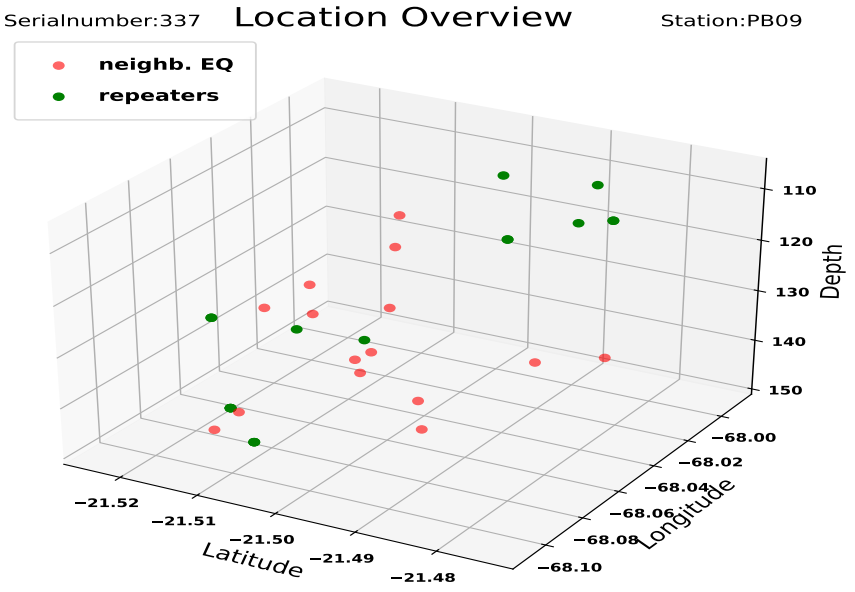
Serialnumber:337
Location Overview
Station:PB09
neighb. EQ
repeaters
Depth
110
120
130
140
150
Longitude
−68.00
−68.02
−68.04
−68.06
−68.08
−68.10
Latitude
−21.52
−21.51
−21.50
−21.49
−21.48

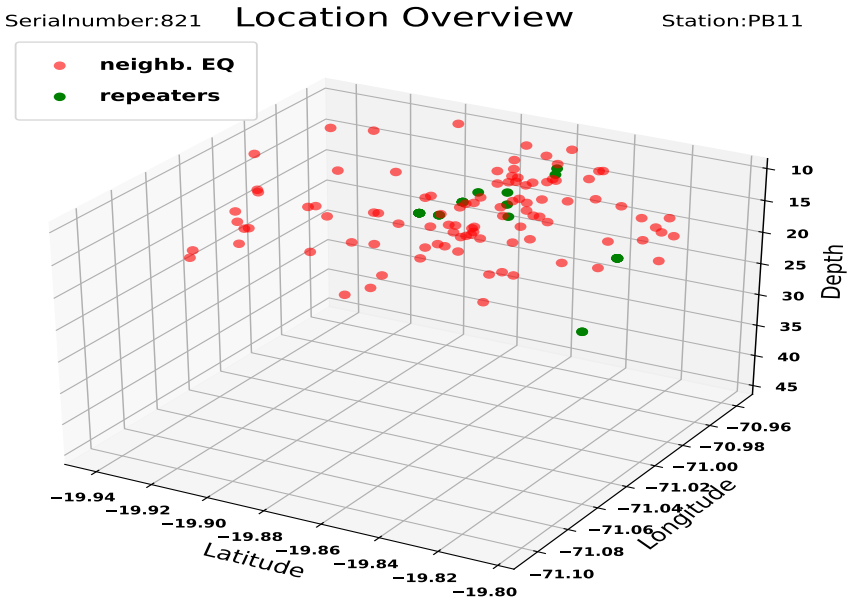
Serialnumber:821
Location Overview
Station:PB11
neighb. EQ
repeaters
Depth
10
15
20
25
30
35
40
45
Latitude
−19.94
−19.92
−19.90
−19.88
−19.86
−19.84
−19.82
−19.80
Longitude
−70.96
−70.98
−71.00
−71.02
−71.04
−71.06
−71.08
−71.10

Bibliography

Beyreuther, M., Barsch, R., Krischer, L., Megies, T., Behr, Y., and Wassermann, J. (2010). Obspy: A python toolbox for seismology. *SRL*, 81(3).

F. Pasten-Araya, P. Salazar, S., E.Rivera, B.Potin, Maksymowicz, A., E.Torres, Villarroel, J., Cruz, E., Valenzuela, J., Jaldín, D., G.González, Bloch, W., Wigger, P., and Shapiro, S. A. (2018). Fluids along the plate interface influencing the frictional regime of the chilean subduction zone, northern chile. *Geophysical Research Letters*.

Gao, D. and Kao, H. (2020). Optimization of the match-filtering method for robust repeating earthquake detection: The multisegment cross-correlation approach. *Journal of Geophysical Research: Solid Earth*, 125.

Husen, S., Kissling, E., Flueh, E., and Asch, G. (1999). Accurate hypocentre determination in the seismogenic zone of the subducting nazca plate in northern chile using a combined on-/offshore network. *Geophys.J.Int.*

Igarashi, T., Matsuzawa, T., and Hasegawa, A. (2003). Repeating earthquakes and interplate aseismic slip in the northeastern japan subduction zone. *Journal of Geophysical Research*, 108.

Julian, B. R. and Anderson, D. L. (1968). Travel times, apparent velocities and amplitudes of body waves. *Bulletin of the Seismological Society of America*, 58.

Kendrick, E., Bevis, M., SmalleyJr., R., and Brooks, B. (2001). An integrated crustal velocity field for the central andes. *Geochemistry, Geophysics, Geosystems*, 2.

Sippl, C., Schurr, B., Asch, G., and Kummerow, J. (2018). Seismicity structure of the northern chile forearc from >100,000 double-difference relocated hypocenters. *Journal of Geophysical Research Solid Earth Solid Earth*, 123.

Sippl, C., Schurr, B., Münchmeyer, J., Barrientos, S., and Oncken, O. (2023). The Northern chile forearc constrained by 15 years of permanent seismic monitoring. *Journal of South American Earth Sciences*, 126.

Uchida, N. (2019). Detection of repeating earthquakes and their application in characterizing slow fault slip. *Progress in Earth and Planetary Science*, 6.

Uchida, N. and Bürgmann, R. (2019). Repeating earthquakes. *Annual Review of Earth and Planetary Sciences*.